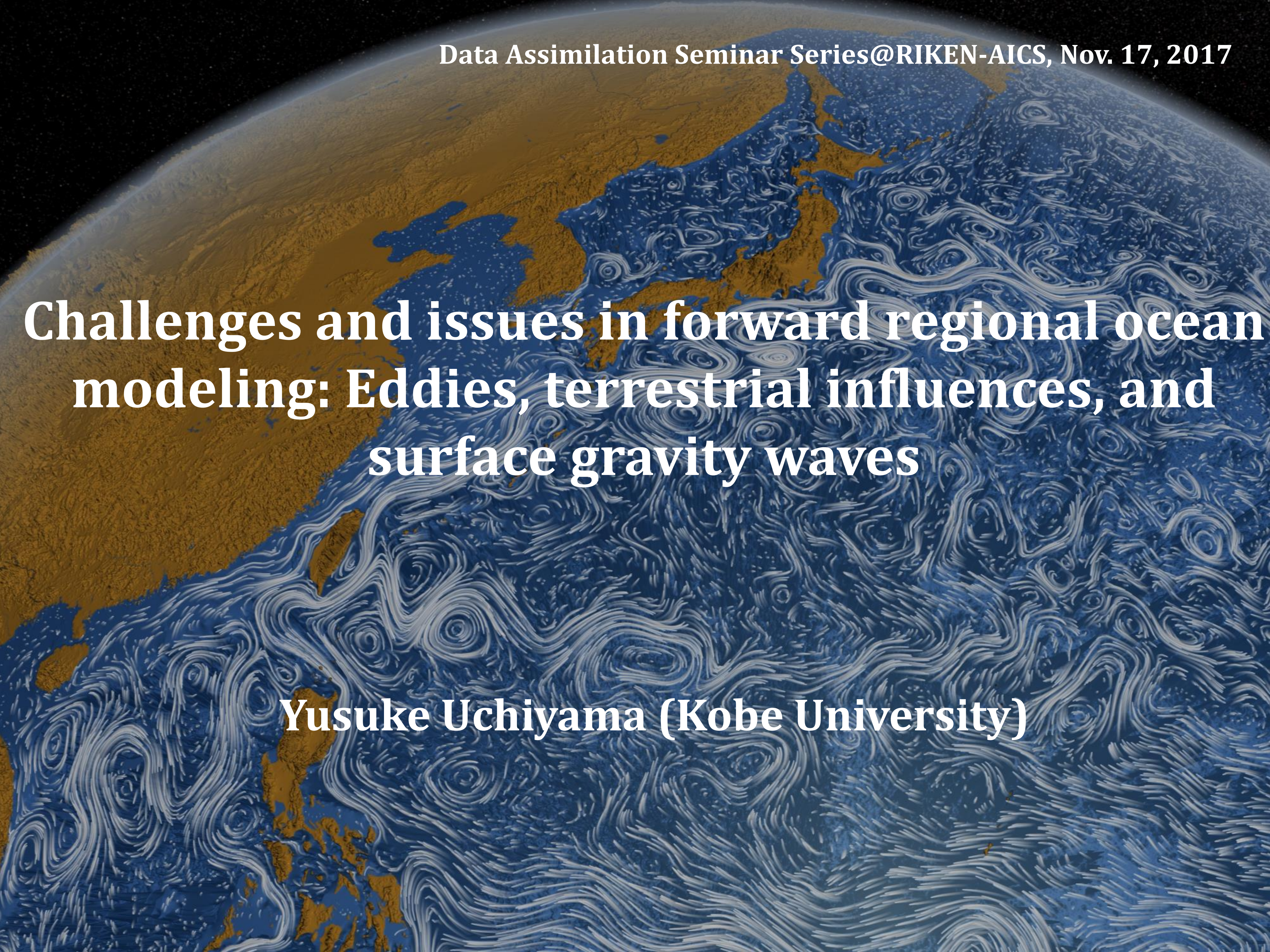

Data Assimilation Seminar Series@RIKEN-AICS, Nov. 17, 2017

Challenges and issues in forward regional ocean modeling: Eddies, terrestrial influences, and surface gravity waves

Yusuke Uchiyama (Kobe University)

Influence of the Gulf Stream on the troposphere

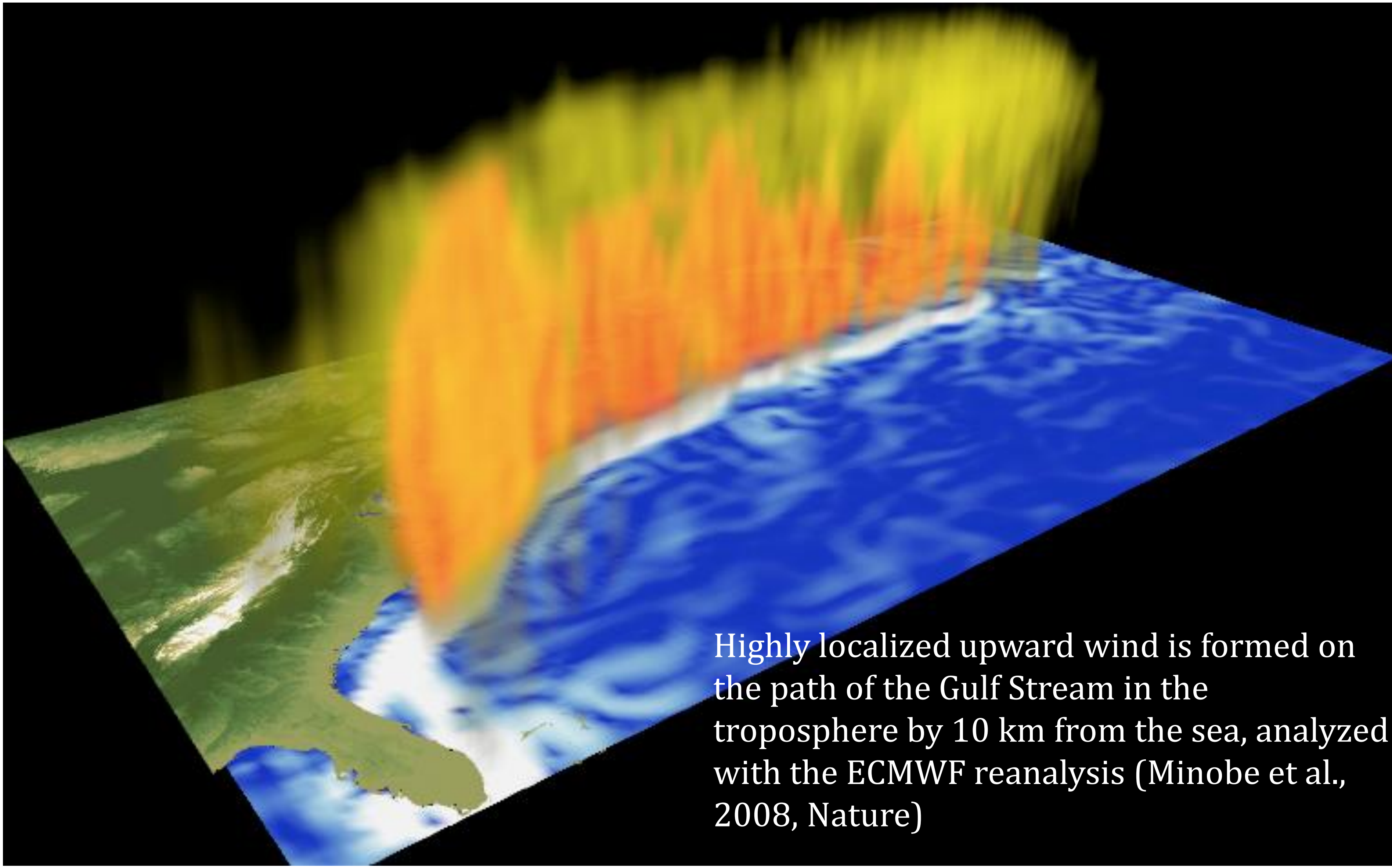

Highly localized upward wind is formed on the path of the Gulf Stream in the troposphere by 10 km from the sea, analyzed with the ECMWF reanalysis (Minobe et al., 2008, Nature)

The Value and Limitations of Oceanic Modeling

- Scientifically, models give high information content and moderate precision.

- In utility, global models have great successes in data-assimilated weather prediction and climate change.

- Ocean models have few large-scale clients (other than climate), but potentially many more coastal ones.

- *Key words*: eddies, terrestrial influences, and surface waves

Eddies

Mesoscale Eddies in North Pacific determined by satellite altimetry (AVISO)

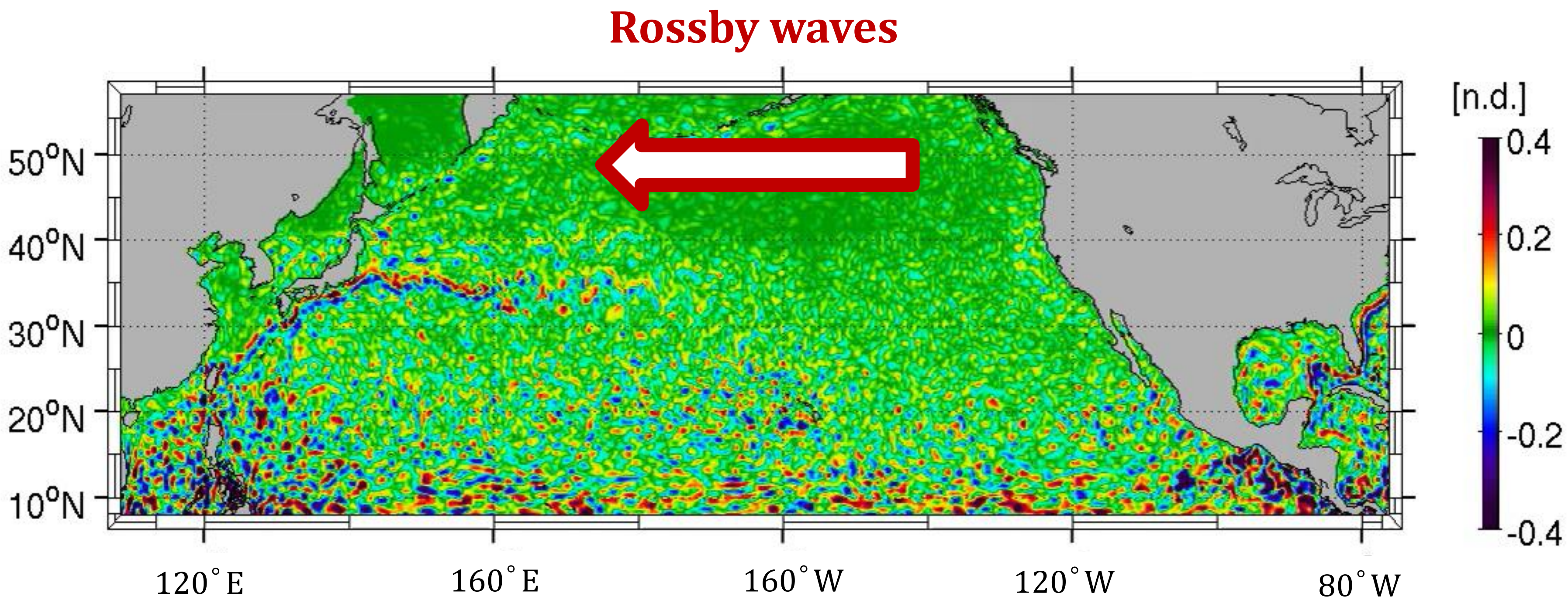

temporal evolution of relative vorticity normalized by f

Uchiyama, Okada, and Kurosawa (2017)

Mesoscale activity in the ocean

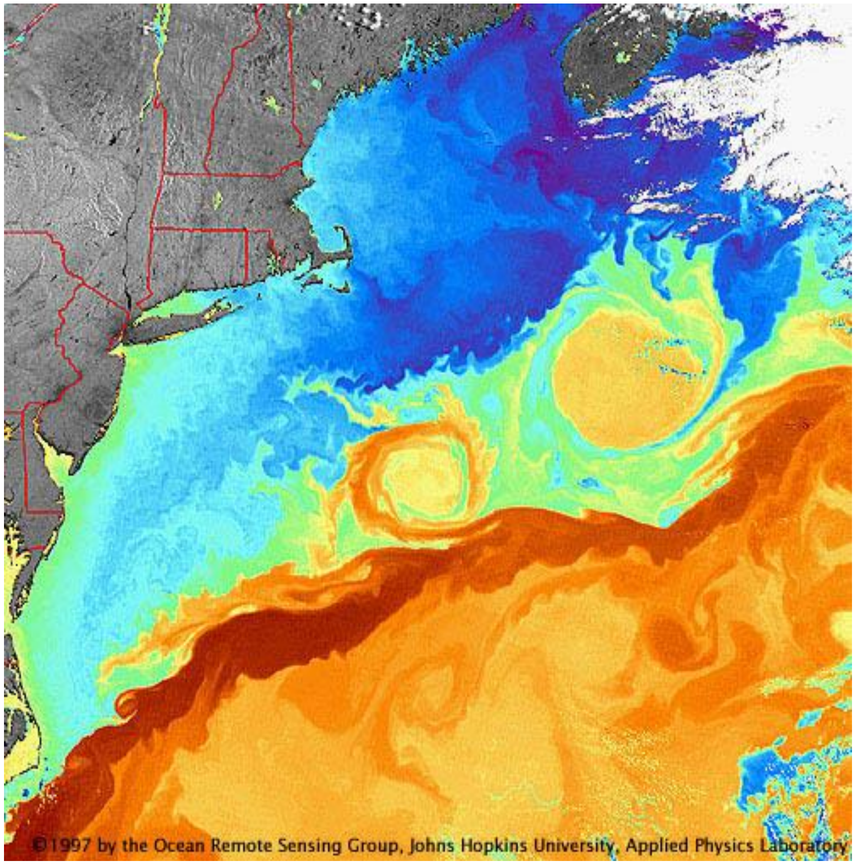

SST off the US East Coast

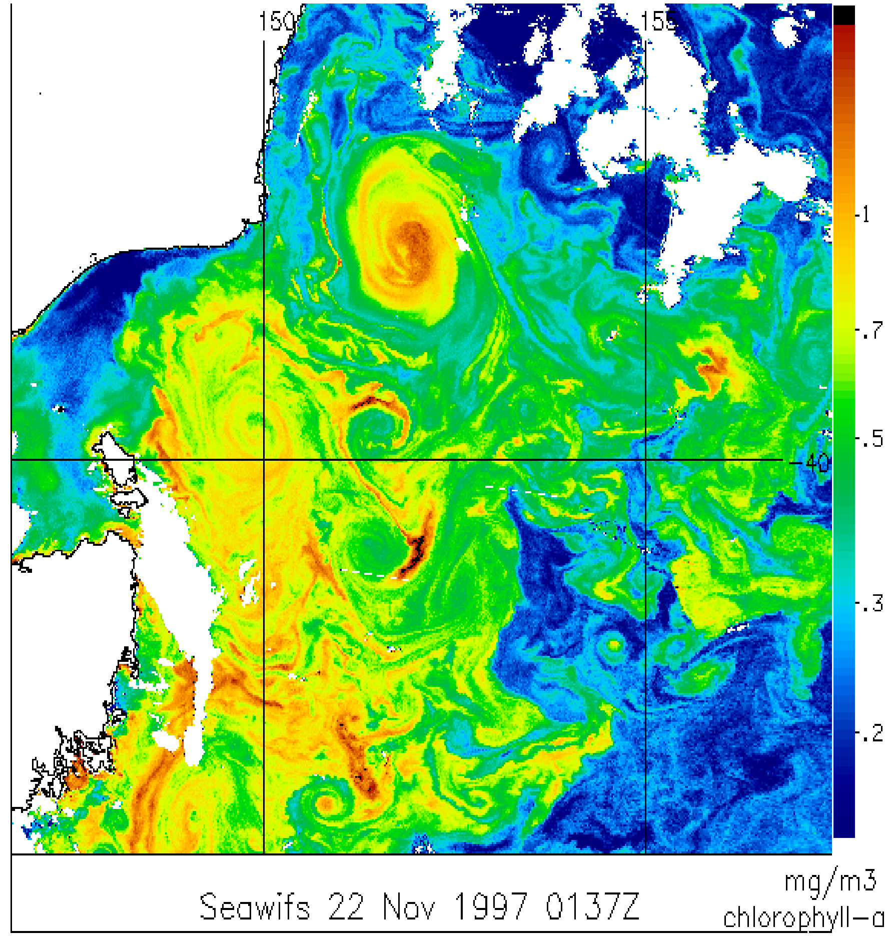

Chl. a off the Eastern Australia

There is a natural length scale (the deformation radius) in stratified rotating fluids that will condition energy distribution and hence tracer appearance.

Mesoscale to submesoscale transition

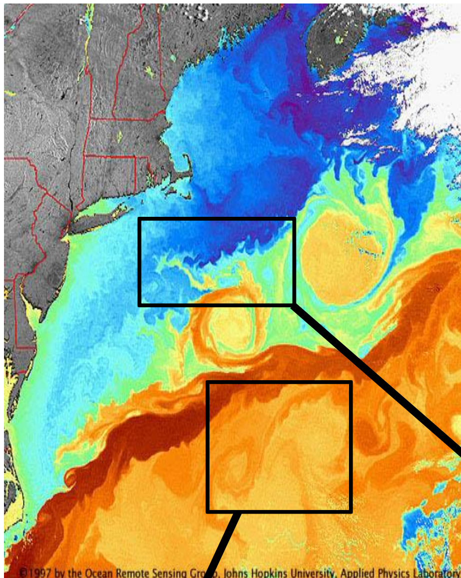

Submesoscale frontal instability

Mesoscale dynamics: *Ro* ($\sim \zeta / f$) << 1, *Ri* >>1

- → mesoscale filaments, fronts, etc..
- → loss of balance
- → ageostrohpic secondary flows (larger *w*)

Transition to submesoscale: *Ro* & *Ri* $\sim O(1)$

$L \sim 30$ km (<< Rossby deformation radius)

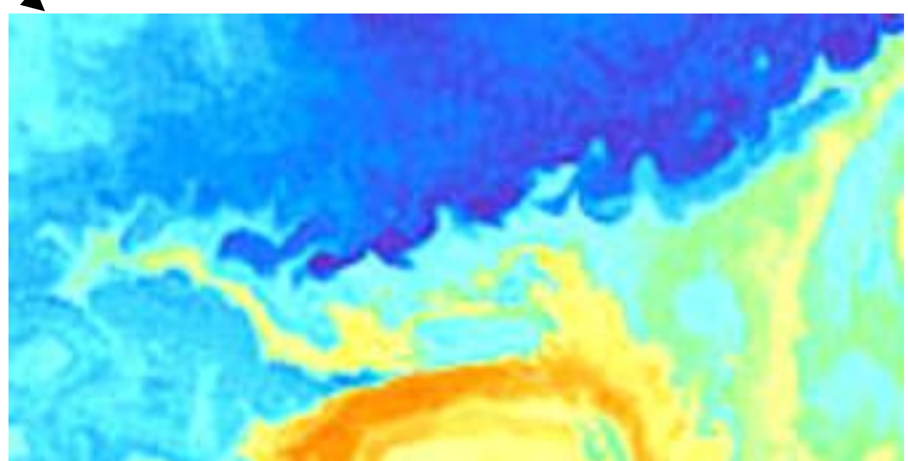

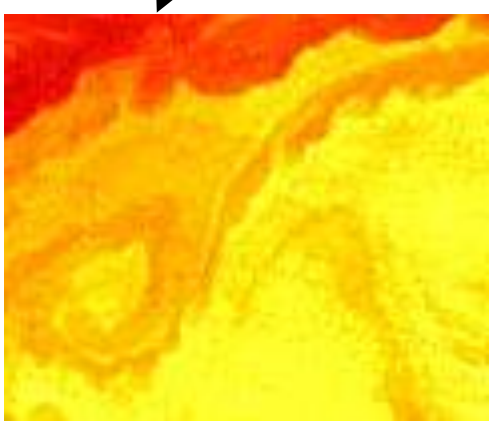

Scaling of Submesoscales

- Rossby number: $Ro = \zeta / f$
  $\zeta \sim U / L$, so $Ro \sim U / f L$ → $L = U / f$

- Submesoscale length scale L in terms of lateral buoyancy gradient b_y
  $U \sim b_y H / f$ (thermal wind balance)
  where $b = - g \rho'/\rho_0$ is buoyancy, and H is mixed-layer depth
  → $L = M^2 H / f^2$, where $M^2 = b_y$

- Submesoscale length scale L in terms of vertical buoyancy gradient b_z
  $b_z = N^2$, at adjusted front scale by b_y: $N^2 = M^4 / f^2$ (Tandon and Garrett, 1994)
  → $L = N H / f$, where N and H are specific to the mixed layer & front

  ex: $H = 50$ m, $N = 10^{-3}$ 1/s, $f = 0.5 \times 10^{-4}$ 1/s
  → $L = 1$ km, $U = 0.1$ m/s, $Ro \sim O(1)$

  Bulk Richardson number $Ri = N^2 H^2 / U^2 = Ro^{-1/2} \sim O(1)$

- Aspect ratio of submesoscale flow: $\Gamma = H/L = f/N << 1$

- Hydrostatic condition: accurate to $O(Ro^2\Gamma) << 1$ → OK at $dx \sim O(0.1 \text{ km})$.

The Value and Limitations of *Submesoscale* Oceanic Modeling

- Submesoscale coastal models are quite new, still with some growing pains to fit all the circulation pieces together and validate them statistically (*n.b.*, intrinsic variability).
- For now, models lead the observations in submesoscale phenomena.
- *Real-time coastal analyses* can be envisioned with mesoscale data assimilation and submesoscale downscaling (*cf*., tornado forecasts). Validated mesoscale skill will be determinative.
- This is a labor-intensive path, as yet without much of a labor force and client base. Faster progress requires a larger consortium.

Double nested JCOPE2-ROMS modeling off Japan

Uchiyama, Ishii, and Miyazawa (2012)

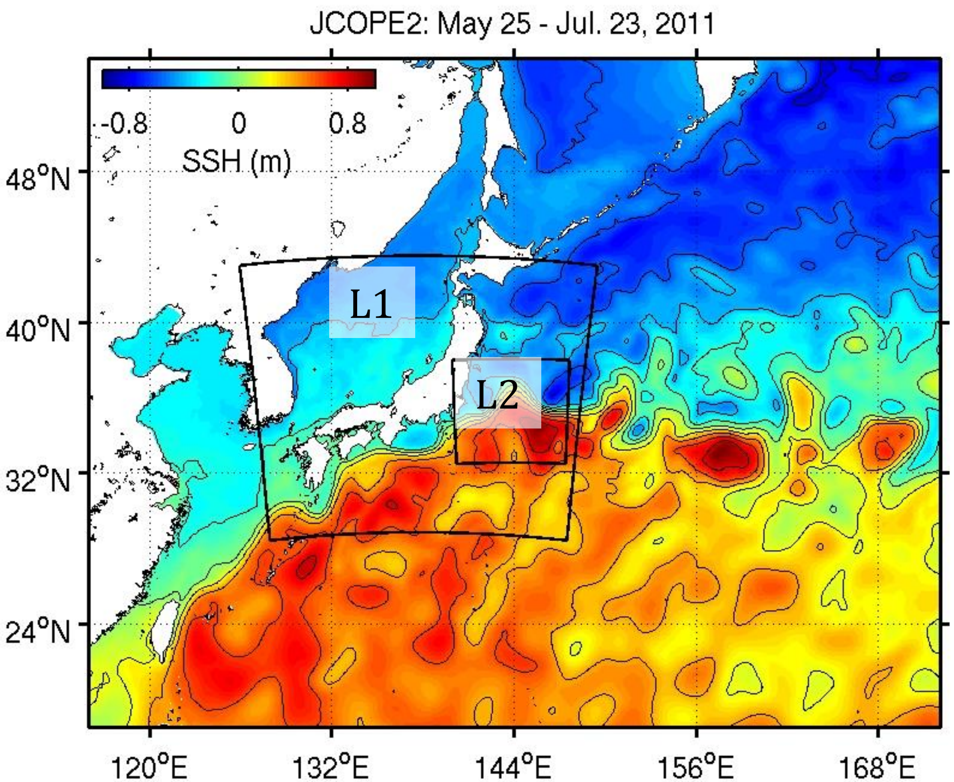

Mean sea surface field from JCOPE2

JCOPE2 (dx ~ 1/12 deg.) → b.c. → L1 (dx ~ 3 km) with TS-nudging → b.c. → L2 (dx ~ 1 km) without any controls

1-way offline nesting is used to accomplish downscaling

L2 configuration

Computational period	Jan. 1, 2003 ~ Jul. 29, 2004
Horizontal grids	672 x 608 (x 40 level)
Surface wind stress	JMA GPV-MSM (hourly)
Other surface flux	COADS (monthly)
SST	Pathfinder-AVHRR (monthly)
Boundary condition	ROMS-L1(3km, daily)
Initial condition	ROMS-L1 (Jan. 1, 2003)
Time step	60 sec.
Topography	JEGG500 and SRTM30

Configurations at 3 km resolution (ROMS-L1)

Three test cases with horizontal resolution of 3 km (ROMS-L1) for 2009 are performed to ensure if flow variation (e.g., meandering patterns and separating latitude, etc.) is generally consistent with that of JCOPE2.

Three cases

1. Without any controls (Free).
2. With a constant horizontal eddy viscosity of 100 m^2/s (Control).
3. With a weak four-dimensional TS-nudging at a relaxation time scale of 20 days towards 10-day averaged JCOPE2 (TCLIM).

Other configurations

Surface wind stress	JMA GPV-MSM（hourly）
Other surface fluxes	COADS (monthly climatology)
Sea surface temp	Pathfinder-AVHRR (monthly climatology)
topography	JEGG500 and SRTM30

Volume-averaged surface (z > -400m) kinetic energy from Jan. 1, 2009 to Jan. 1, 2010.

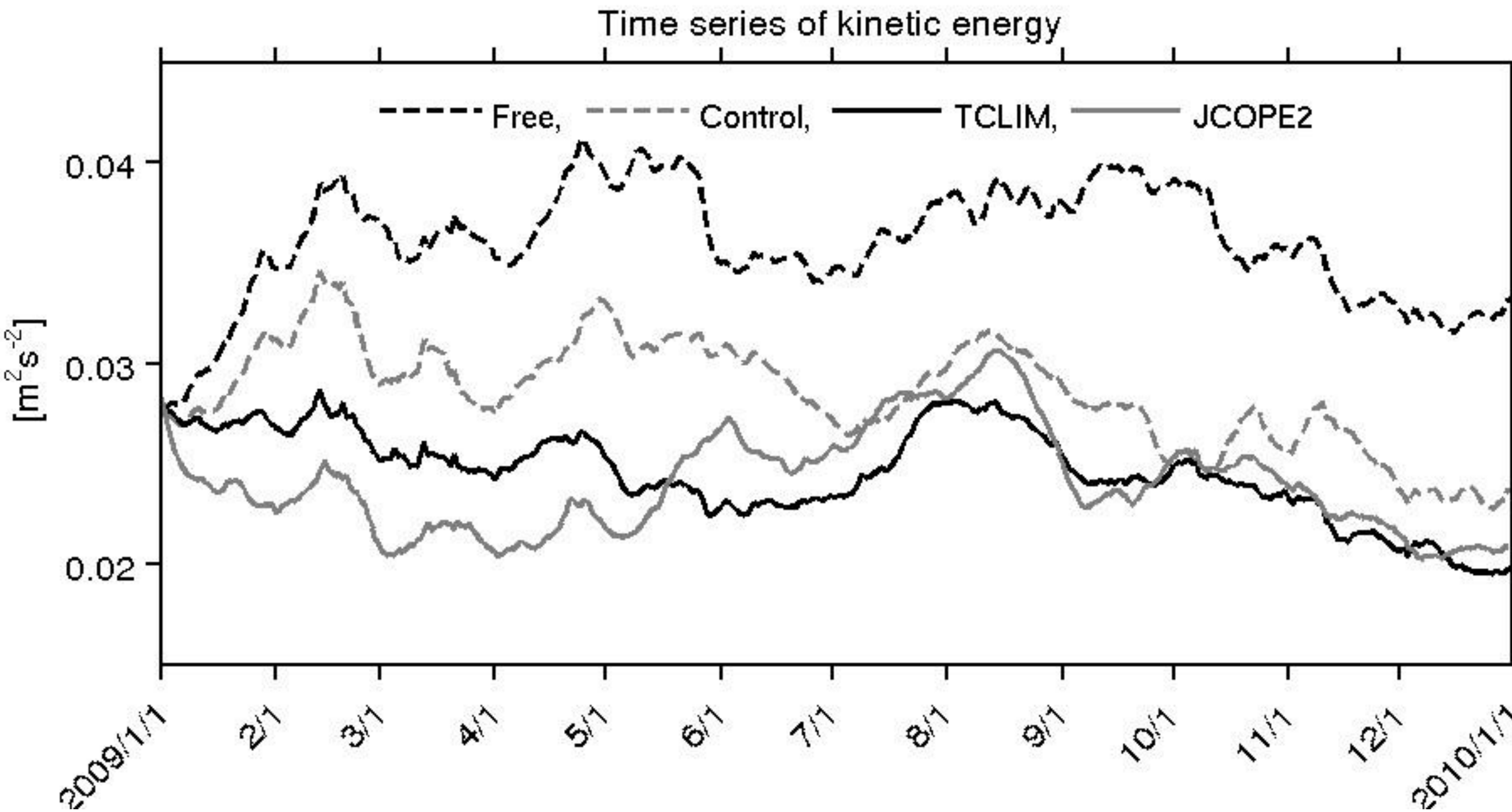

In case without any controls (Free), Kuroshio paths excessively fluctuate. Furthermore this case substantially overestimates the KE and EKE compared with JCOPE2 because of lack of subgrid-scale energy dissipation.

Cross-sectional seasonally mean data comparing with JMA climatology along 137E line (left : ROMS-L1, right : JMA)

Salinity[PSU]

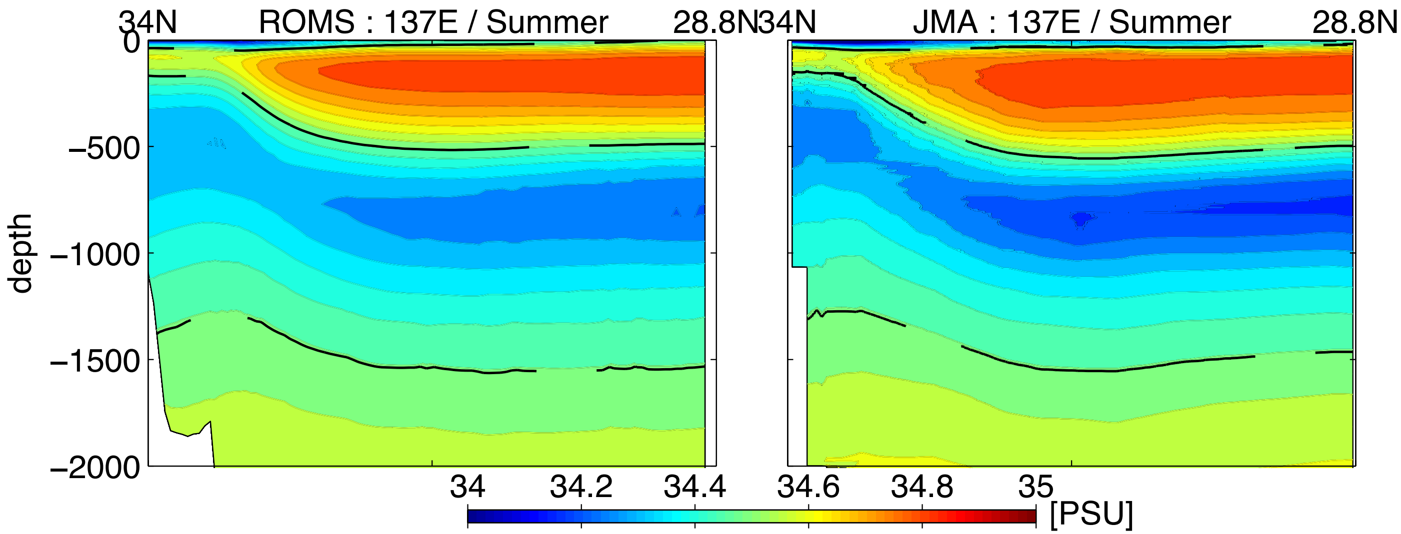

Temperature [°C]

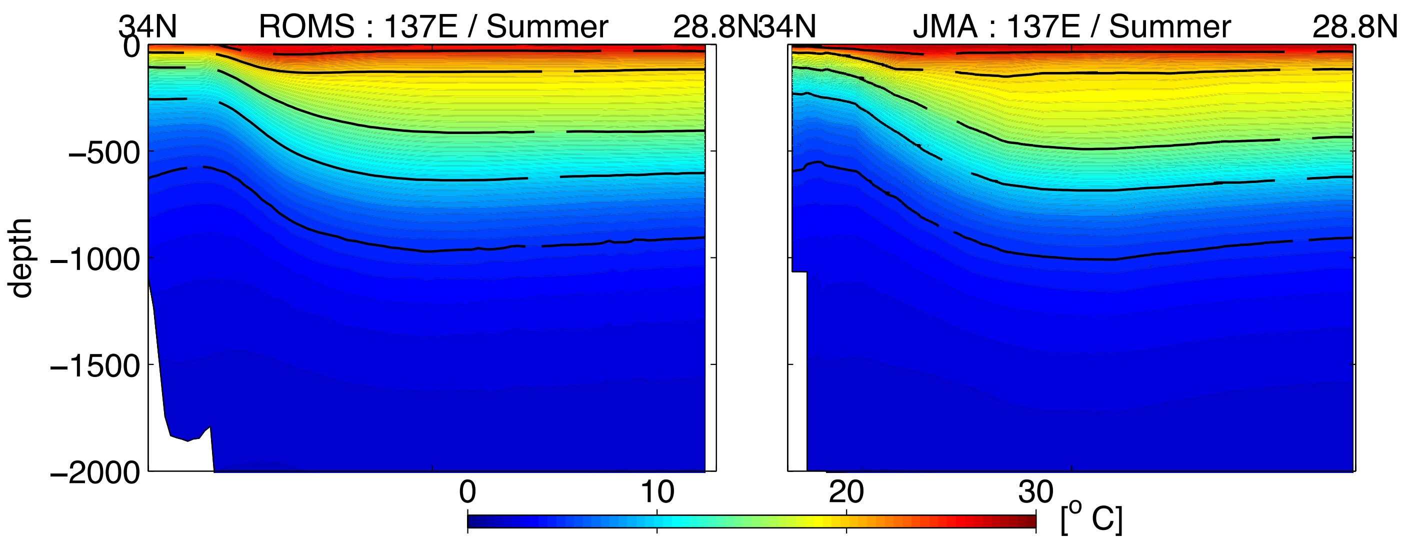

Volume averaged surface kinetic energy (z > -400m) from Jan. 1, 2003 - Nov. 1, 2004

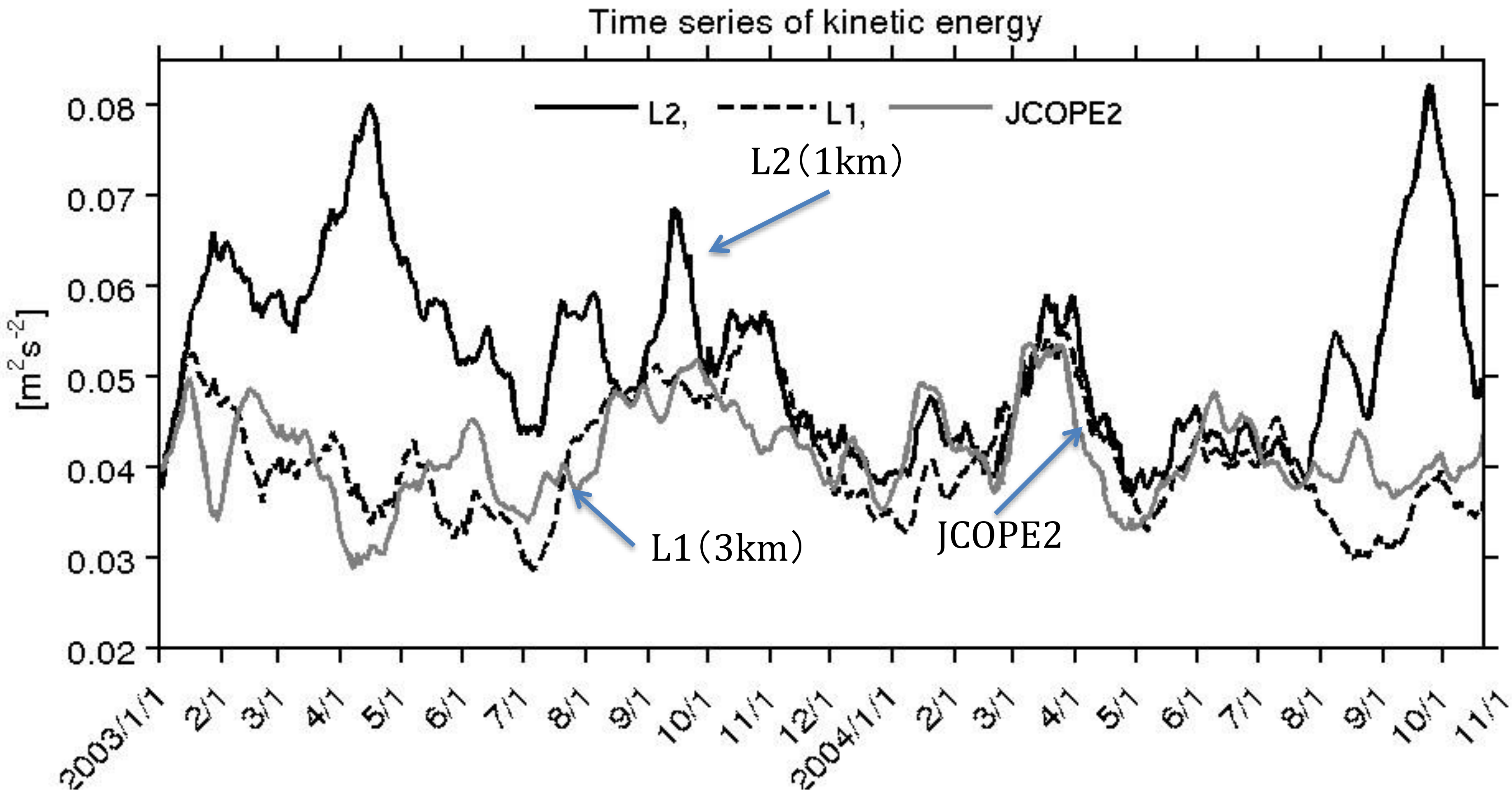

Downscaling effects: horizontal resolution vs. eddies

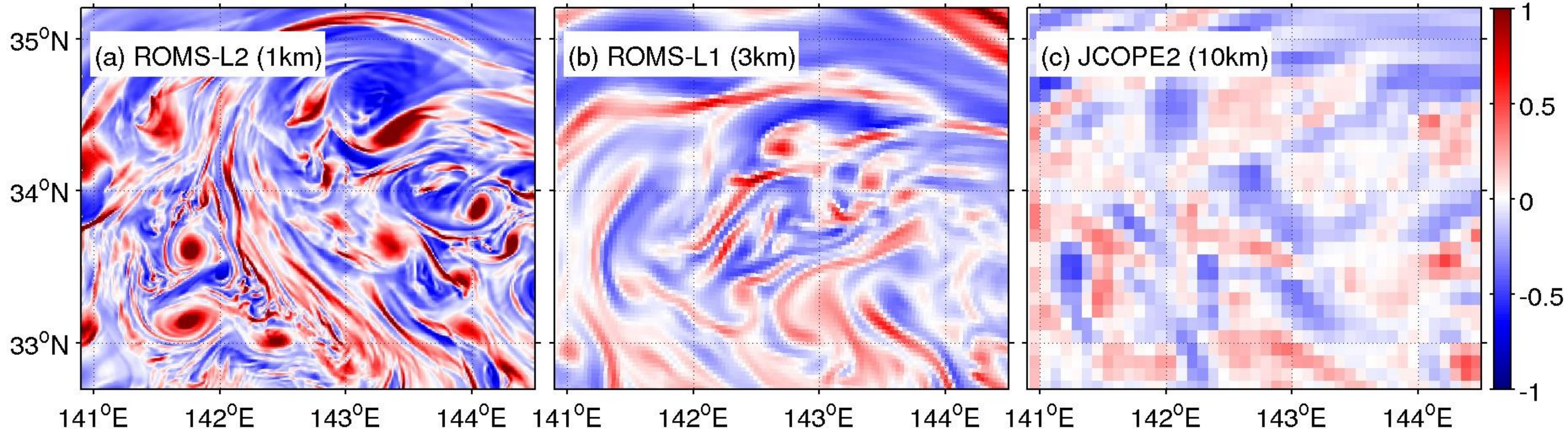

Instantaneous spatial distribution patterns of surface relative vorticity

As resolution increases, strong vorticity associated with submesoscale activities occurs.

Submesoscale-resolving dynamically changes oceanic structures.

Relative dispersion

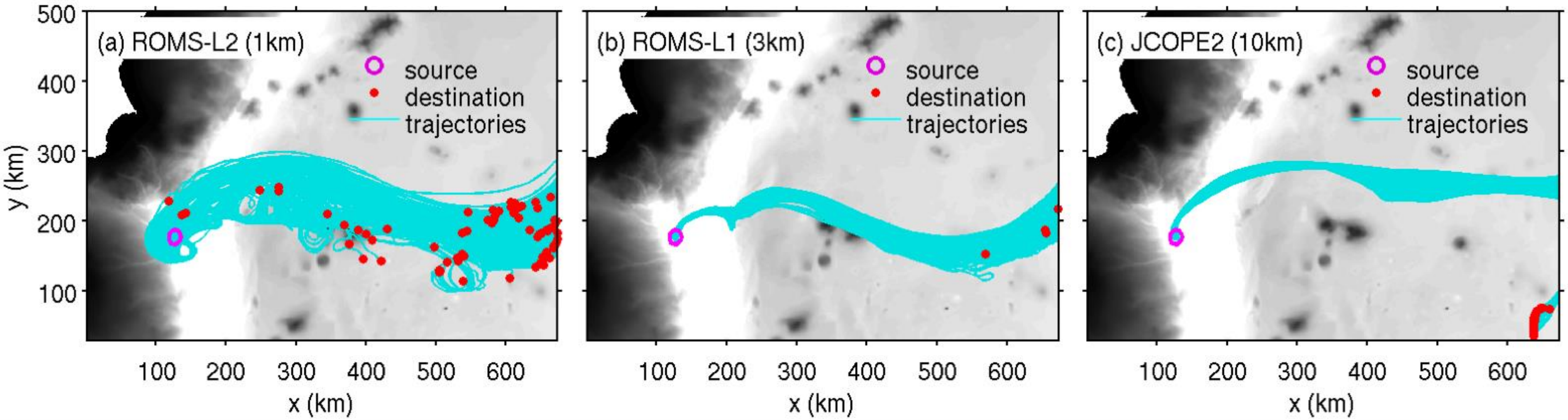

Particle trajectories (after 20 days)

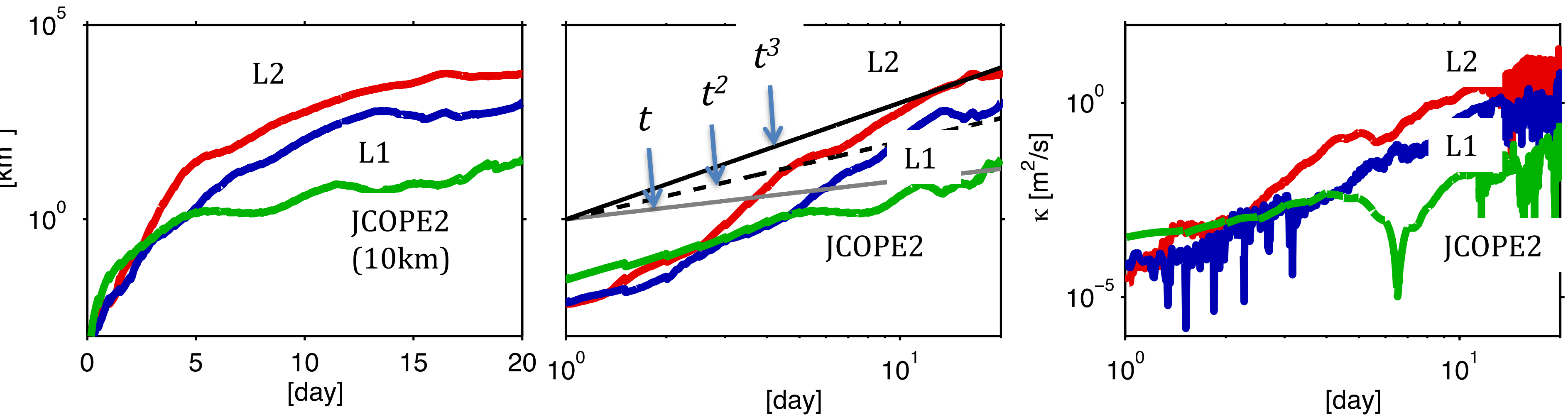

Pair separation squared R^2 (km^2) R^2 log scale (km^2) Relative diffusivity $\varkappa$ (m^2/s)

R^2 curve on L2 converges to t^3, corresponding to Richardson's scaling.

Eddy kinetic energy from computational average

ROMS-L2 (1km) ROMS-L1 (3km) AVISO (1/3 deg.)

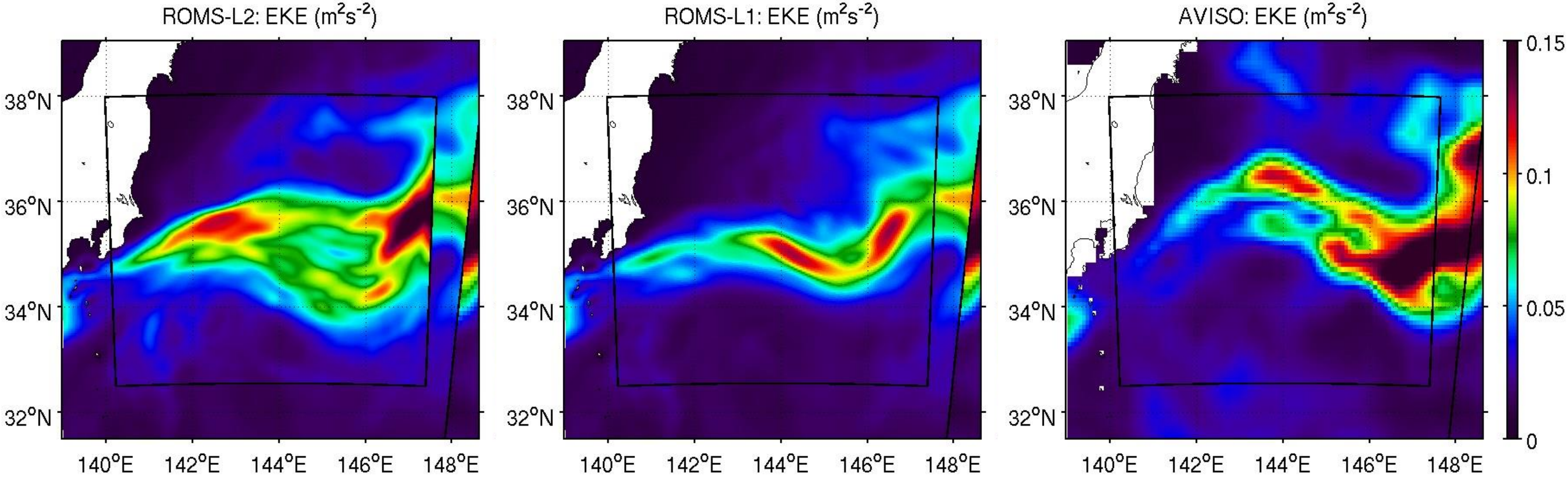

Instantaneous normalized vorticity and EKE at surface

L1（3km） L2（1km） JCOPE2（1/12 deg.）

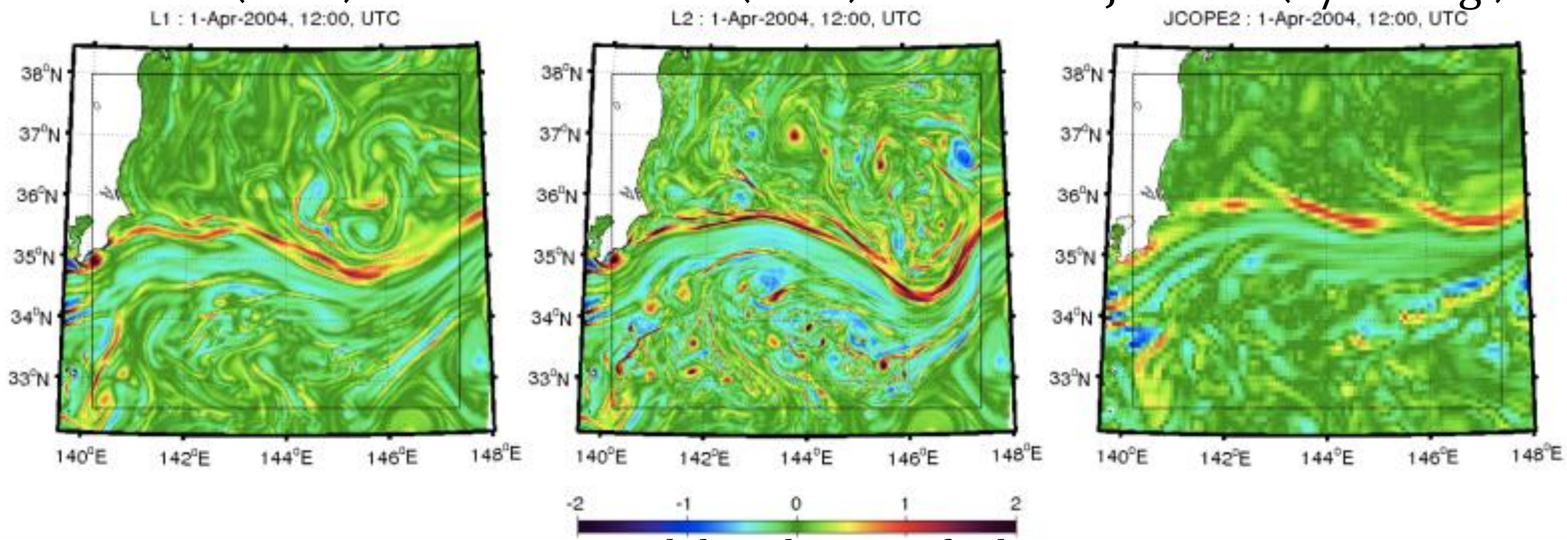

Instantaneous spatial distribution of relative vorticity.

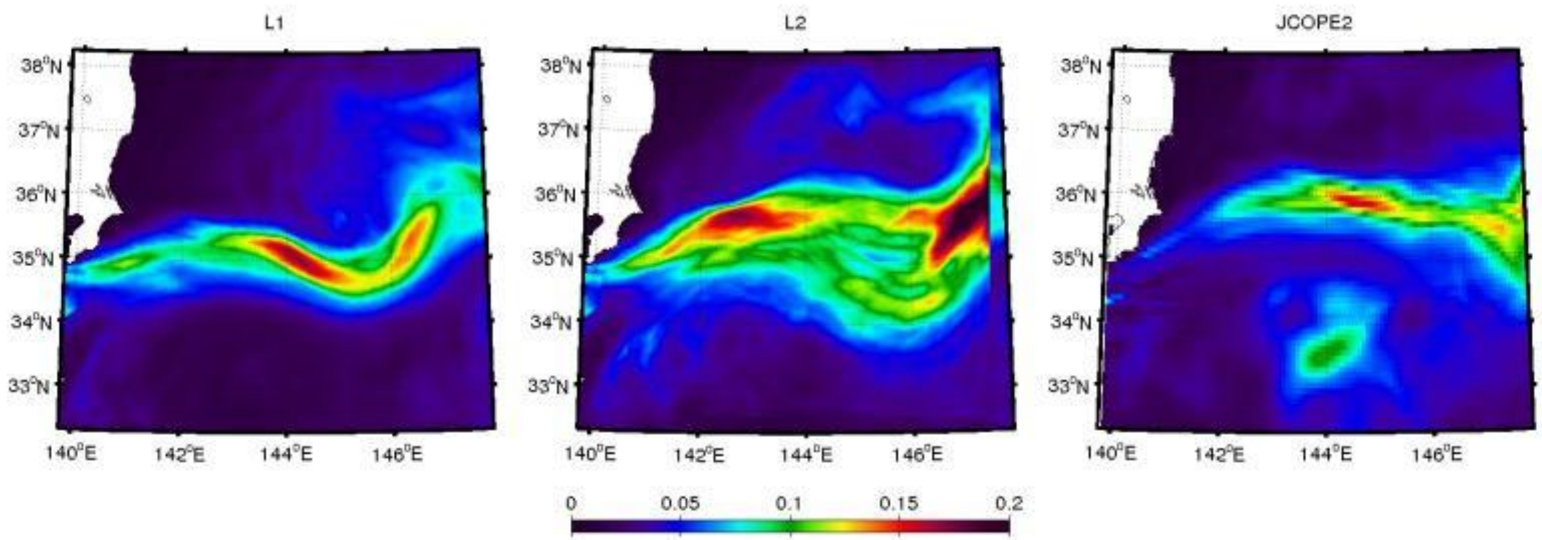

surface EKE

Terrestrial influences

Effects of 14 major rivers (ex. Sendai Bay)

with rivers　　　　w/o rivers

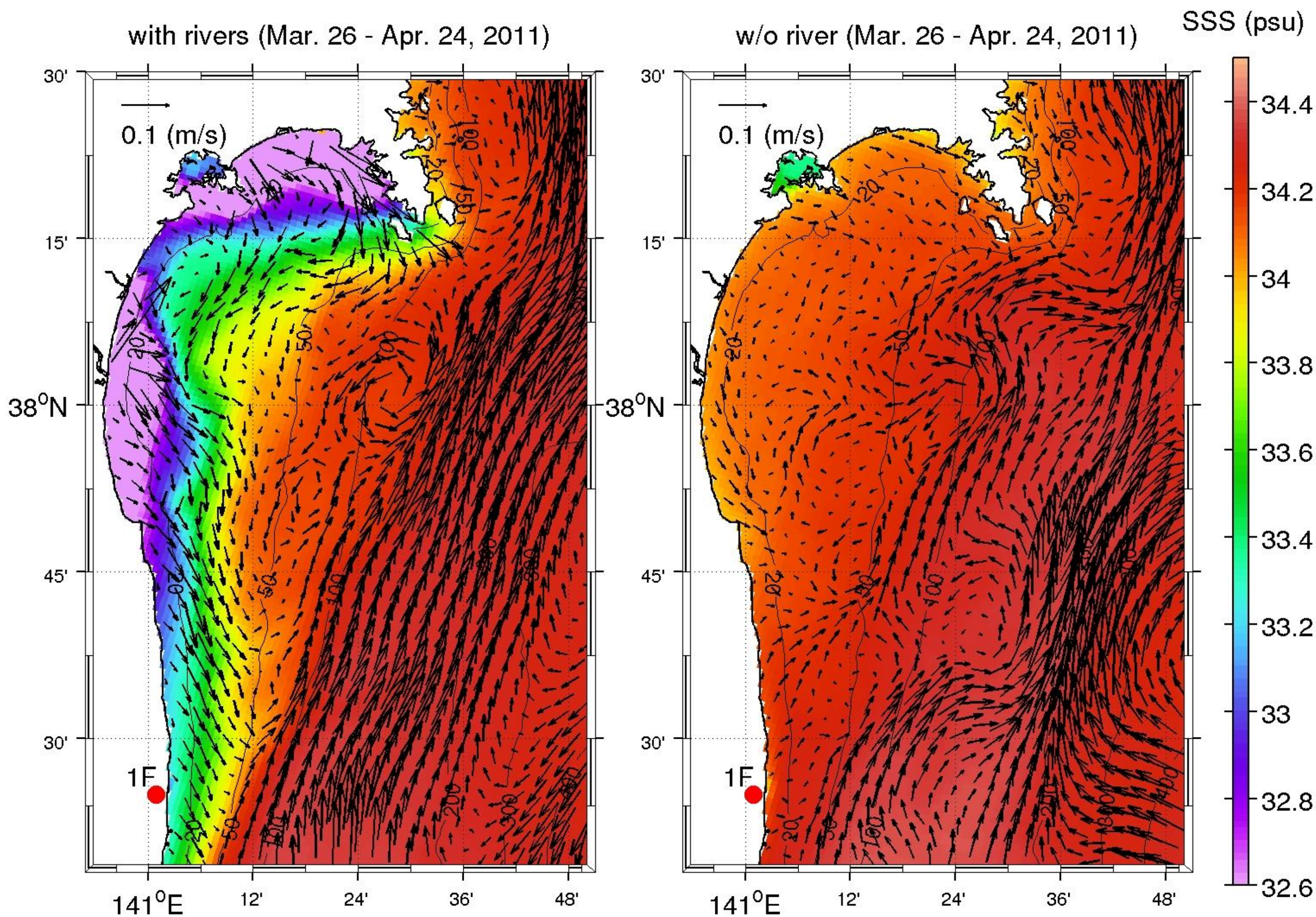

SSS (color) & surface velocity (vectors)

Averaged for 3/26 – 4/24

Offshore transport by rivers

Equatorward riverine water concentrates in a narrow coastal strip

Uchiyama *et al.* (2012)

High-resolution Coastal Model with 3DVAR

An Increasing number of satellite data and Argo floats available for a data assimilation (DA) technique has enabled us more accurate numerical oceanic reanalysis and forecasts. However, this is not always the case in small harbors and estuaries such as the Seto Inland Sea (SIS), Japan, because the data available for DA is desperately limited. In the present study, we develop a 3DVAR system for Regional Oceanic Modeling System (ROMS) and apply to the high-resolution SIS model in a double nested configuration (Kosako *et al.*, 2015) with the publically available *in-situ* data sets.

The primary objectives of the present study are

(1) to investigate a theoretical framework of the 3DVAR algorithm optimal for the high resolution configuration,
(2) to couple the developed 3DVAR with the SIS ROMS model,
(3) to confirm the effects of ROMS-3DVAR by observational systems simulation experiments (OSSE), and
(4) to validate the model outcomes with the observation.

Double nested Seto Inland Sea modeling based on the JCOPE2-ROMS system

Uchiyama *et al*. (2012; 2014), Kosako *et al*. (2015), Kurosawa *et al*. (2017)

Computational period	**Jan. 1, 2013 – Jan. 31, 2014**
Model grids	**480 × 800 x 32 vertical s-layer, *dx* = 600 m**
Surface wind stress	**JMA GPV-MSM (hourly)**
Surface fluxes	**COADS05 (monthly climatology)**
SST, SSS	**JCOPE2 (20 day-average, flux correction)**
Tide along perimeters	**TPXO7.1, 10 major constituents**
River discharge	**24 major rivers (monthly climatology)**
Topography	**J-EGG500 and SRTM30_PLUS (blended)**
Boundary condition	**ROMS-L1 (*dx* = 2km, daily)**

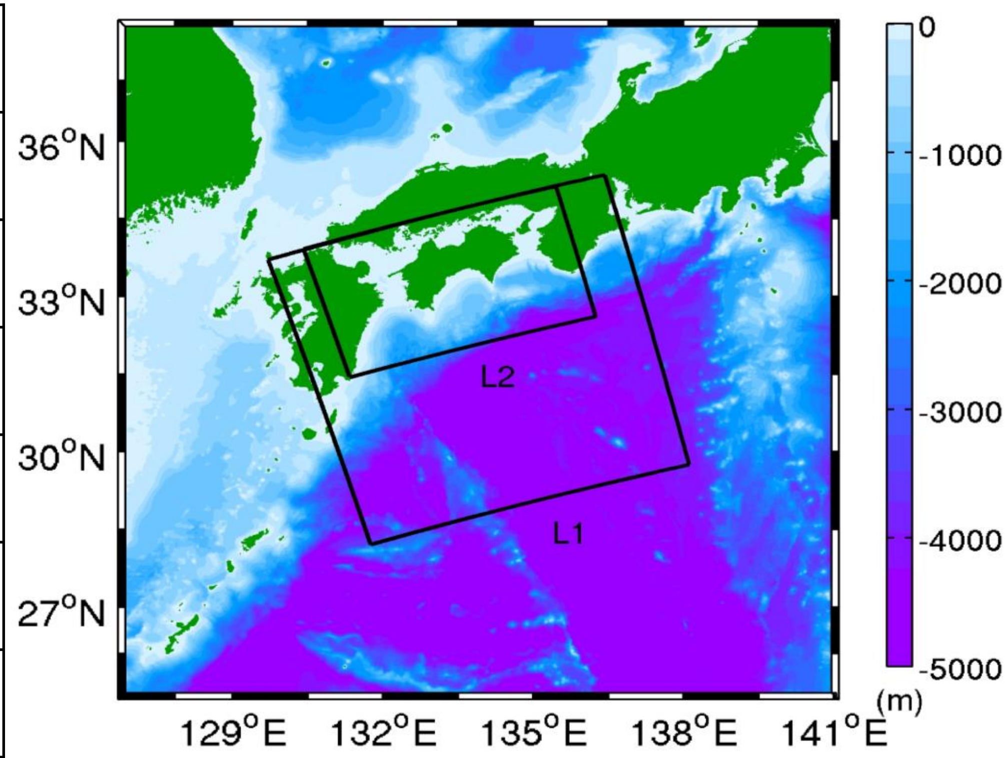

The assimilated in-situ dataset

2013 Seto Inland Sea Comprehensive Water Quality Survey

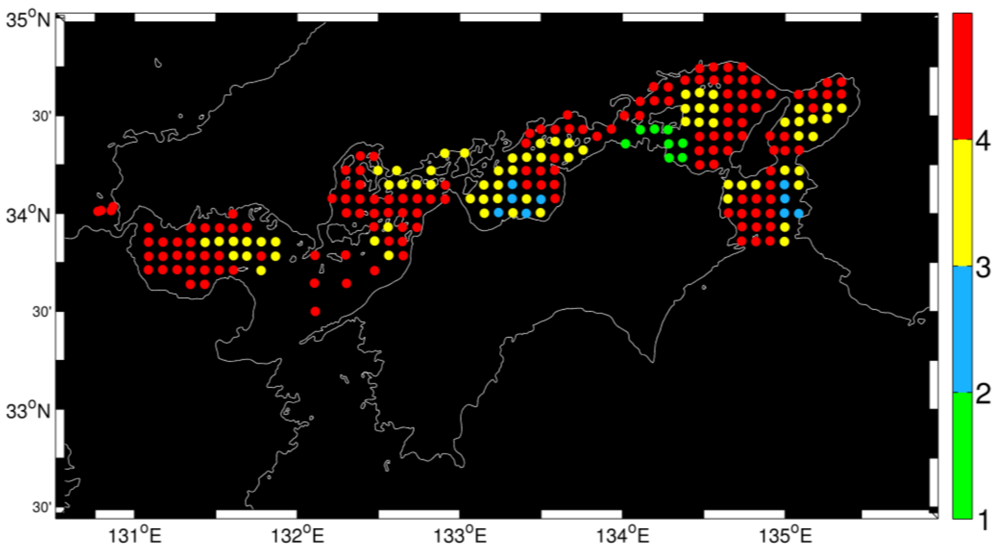

Locations of sampling in 2013

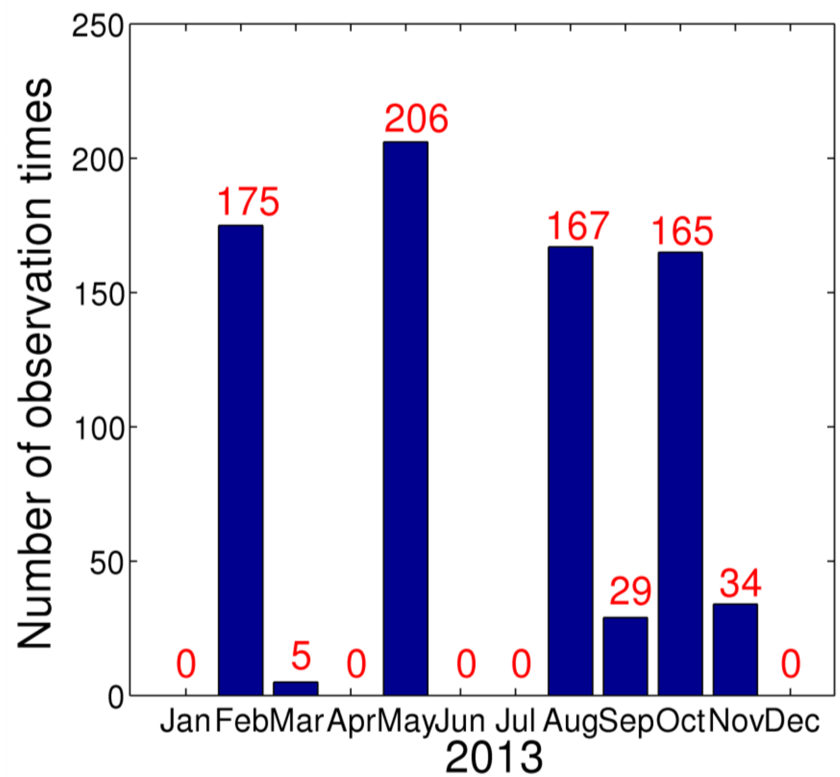

Monthly occurrences of sampling in 2013

Scatter diagram of temperature and salinity.

All the observed data used for 3DVAR vs. the corresponding forecasted results

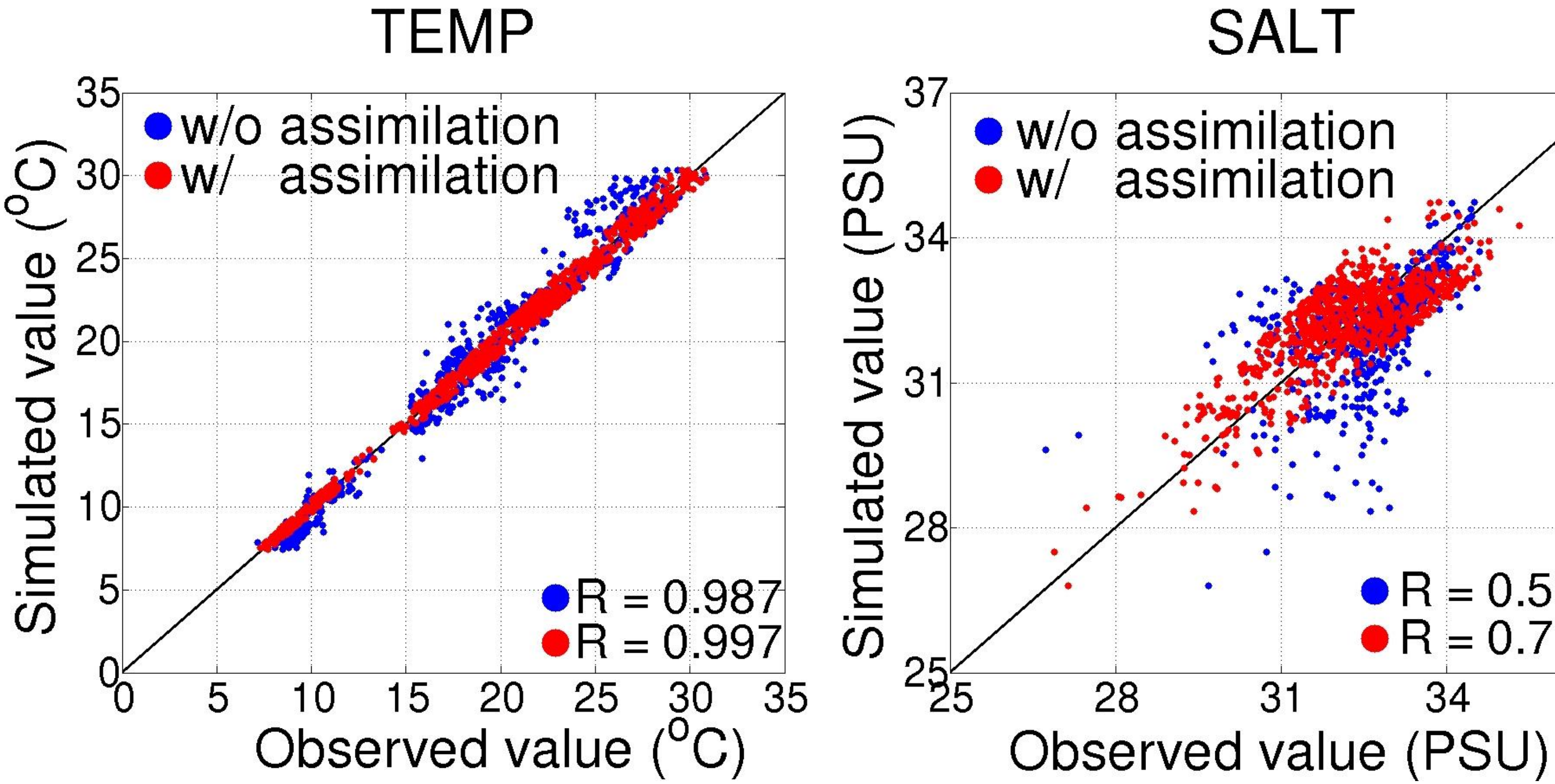

R: correlation coefficient

Kurosawa, Uchiyama and Miyoshi (2017)

Monthly RMSE of the forecasted (left) temperature and (right) salinity against the coinciding observations.

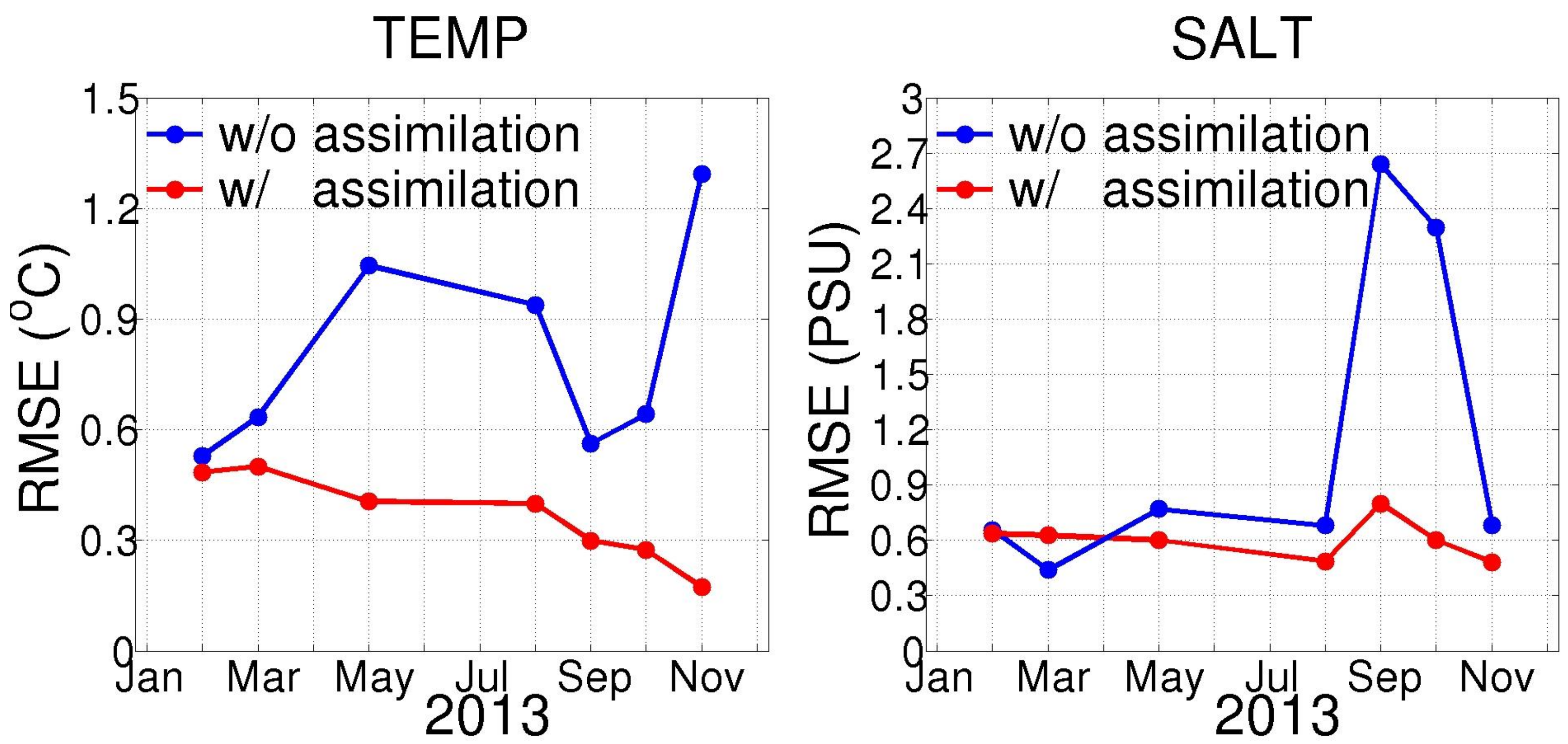

Salinity is not improved as much as water temperature. This is because the model considers only the first class (major) rivers, while they contribute to only ½ of the total freshwater input to the SIS. Therefore, accurate freshwater inflow information is requisite for more successful modeling.

Improvement of SST

MODIS (not used for 3DVAR) | **with 3DVAR** | **w/o 3DVAR**

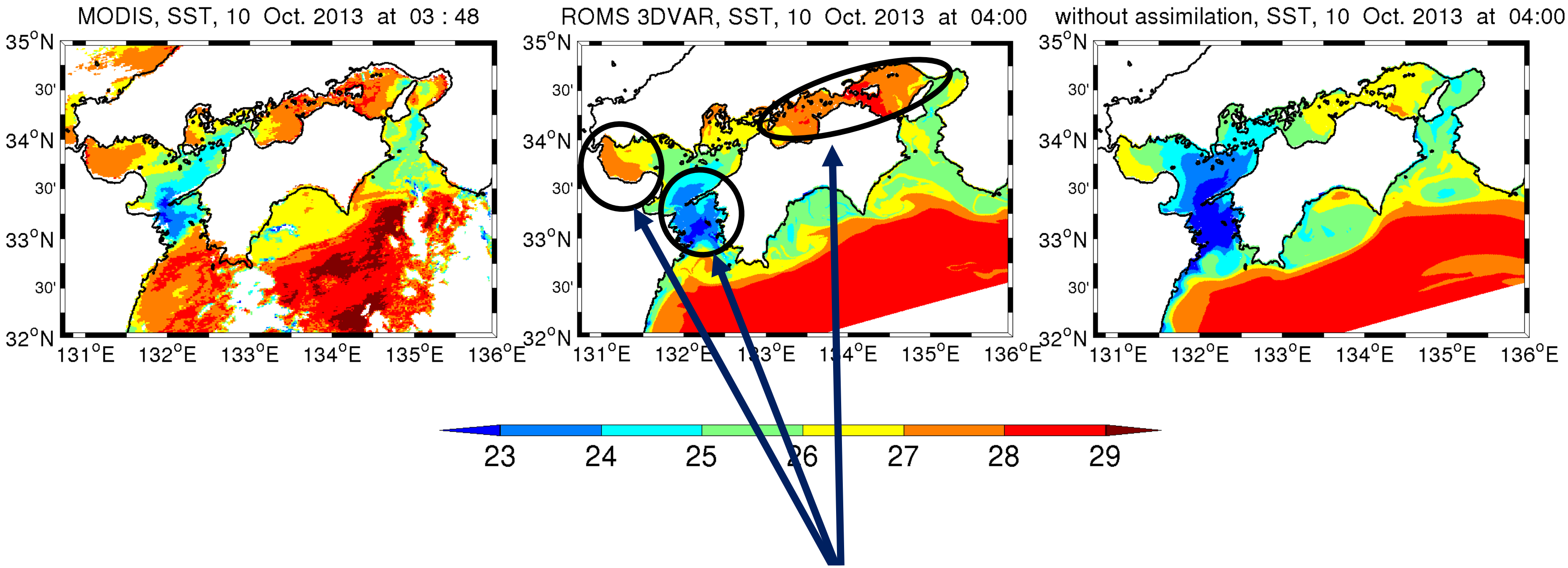

Improved !!!

Surface gravity waves

Photo: S. Henderson (WSU Vancouver)

Rip currents in surf zone

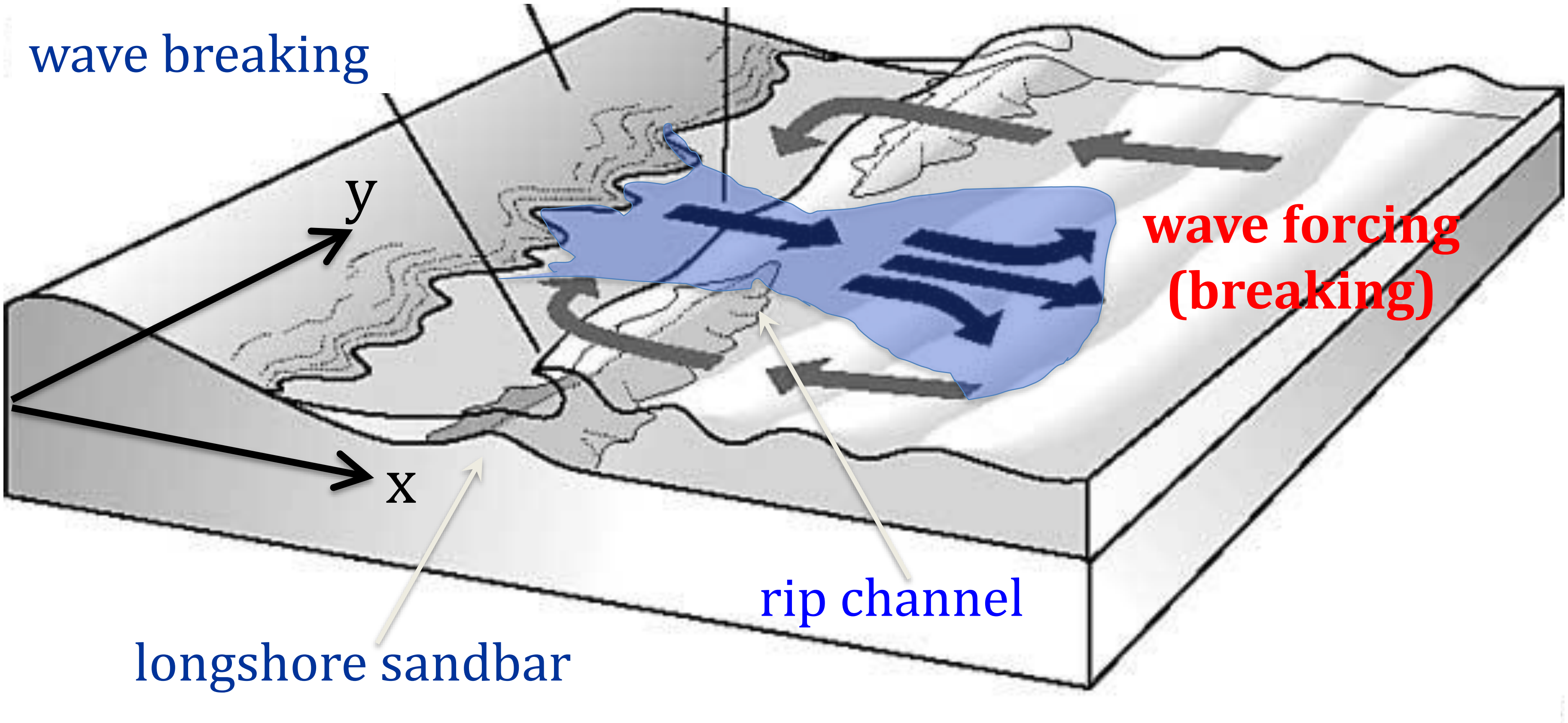

Cross-shore BT momentum balance: wave forcing = $-g\,\eta_x$

Alongshore BT momentum balance: $v_t = -g\,\eta_y$

3-D wave-averaged Primitive Equation

$$\frac{\partial \mathbf{U}}{\partial t} + \underline{\mathbf{U} \cdot \nabla \mathbf{U}} + \frac{1}{\rho_0}\nabla p - \mathcal{B}\mathbf{z} + f\mathbf{z} \times \mathbf{U} = 0.$$

$$\mathbf{U} \cdot \nabla \mathbf{U} = \nabla \cdot (\mathbf{U}\mathbf{U}) + \mathbf{U}(\cancel{\nabla \cdot \mathbf{U}}),$$

Vortex force:

$$\mathbf{U} \cdot \nabla \mathbf{U} = \underbrace{\nabla \frac{|\mathbf{U}|^2}{2}}_{\text{Bernoulli head}} + \underbrace{(\nabla \times \mathbf{U}) \times \mathbf{U}}_{\text{vortex force (VF)}},$$

$U = U_c + U_w$

decomposition (currents and waves)

- waves: weakly nonlinear physics with optical geometry (WKB) approximation
- $U_L = U_E + U^{st}$ (Stokes drift), → choice of reference frame
- 3-D Lagrangian averaging : GLM (Andrews & McIntyre, 1978), thickness-weighted LM (Mellor, 2003, 2005, 2008; Aiki & Greatbatch, 2012)
- 3-D Eulerian averaging: a multi-scale asymptotic theory (McWilliams *et al*., 2004) → prognostic variables: Eulerian, suitable to ocean models/observation
- *vortex force (VF) formalism* (e.g., Craik & Leibovich, 1976) cleanly separates conservative (VF, Bernoulli head, ...) and non-conservative (breaker, streaming, ...) wave effects

ROMS-WEC: Wave-Averaged Primitive Equation

conservative WEC *non-conservative WEC*

Horizontal momentum equation:

$$\underbrace{\frac{\partial \mathbf{u}}{\partial t} + (\mathbf{u}\cdot\nabla_\perp)\mathbf{u} + w\frac{\partial \mathbf{u}}{\partial z} + f\hat{\mathbf{z}}\times\mathbf{u} + \nabla_\perp\phi - \mathbf{F}}_{\text{usual non-wave terms}} = \boxed{-\nabla_\perp\mathcal{K} + \mathbf{J}^{VF} + \mathbf{J}^{SC}} + \boxed{\mathbf{B}^{b} + \mathbf{B}^{wd} + \mathbf{D}^{w}}$$

Bernoulli head

vortex force (VF)

Stokes-Coriolis

breaker acceleration

bottom streaming

...nhanced ...l mixing

...ns

For detail, see Uchiyama, McWilliams and Sh...

WEC: wave effects on currents

CEW: current effects on waves

Ac... l (SWAN/WW3, or WKB ray model) or Data

primary wave action:

$$\frac{\partial \mathcal{A}}{\partial t} + \nabla_\perp\cdot\left[\mathcal{A}\left(\mathbf{C}_g + \bar{\mathbf{u}}\right)\right] = -\frac{\boxed{\epsilon^{b}}}{\sigma} - \frac{\boxed{\epsilon^{wd}}}{\sigma}$$

breaker dissipation

wave-drag dissipation

wave action + wavenumber → conservative WEC

dissipation → non-conservative WEC acceleration

Transient 3-D rip currents

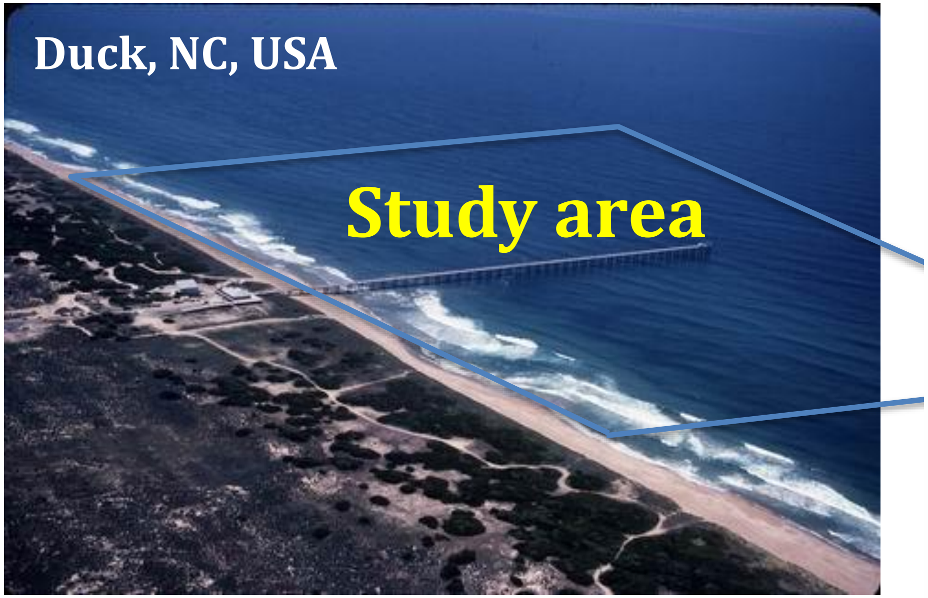

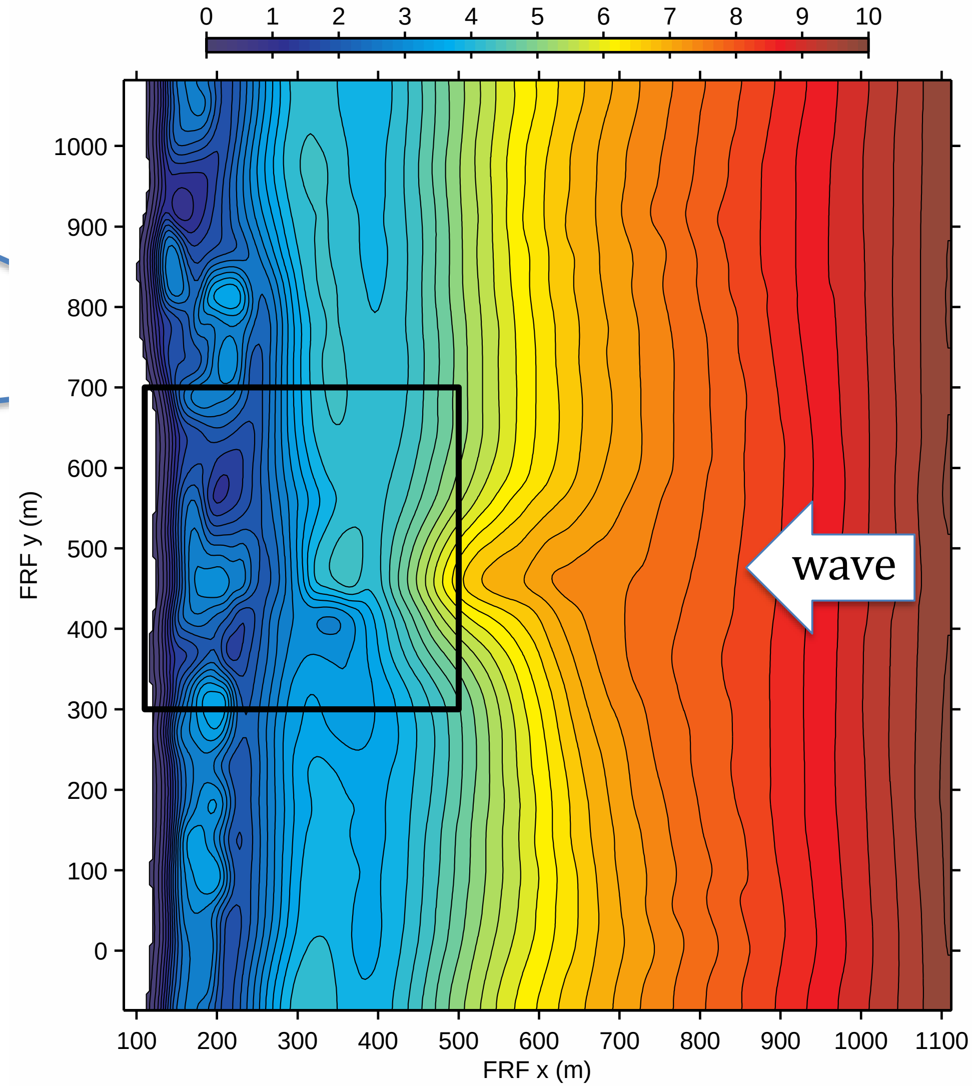

- ✓ $\Delta x = \Delta y = 4$ m
- ✓ 1024 m x 1152 m, 20 vertical layers
- ✓ $H_{rms} = 1.2$ m, $T_p = 10$ s, $\theta_p = 0^o$ (normal incident)
- ✓ The model is forced only by ***STEADY WAVES***. No wind, no tide, no stratification, etc.
- ✓ WEC + CEW config. (Yu and Slinn, 2003, JGR; Weir *et al*., 2011, JGR)

Model topography based on the bathymetry survey on 2/22/2010.

turbulent rip currents: barotropic relative vorticity

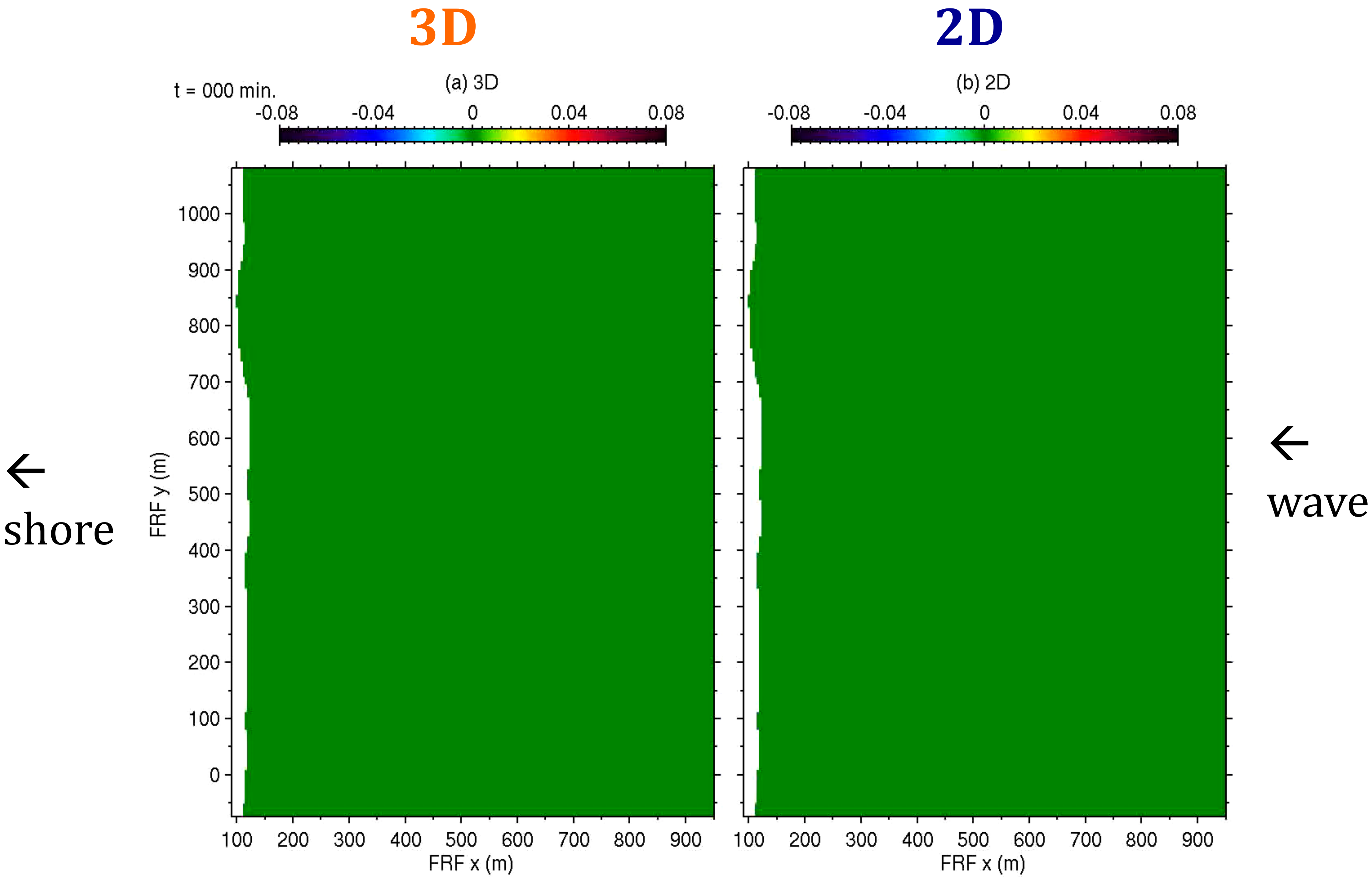

A snap shot of 3D eddies near the rip channel

t = 299 min.

Color: barotropic relative vorticity with the color scale shown above

Thin contours: bathymetry at 1 m intervals

Velocity vectors
-black: surface
-red: bottom

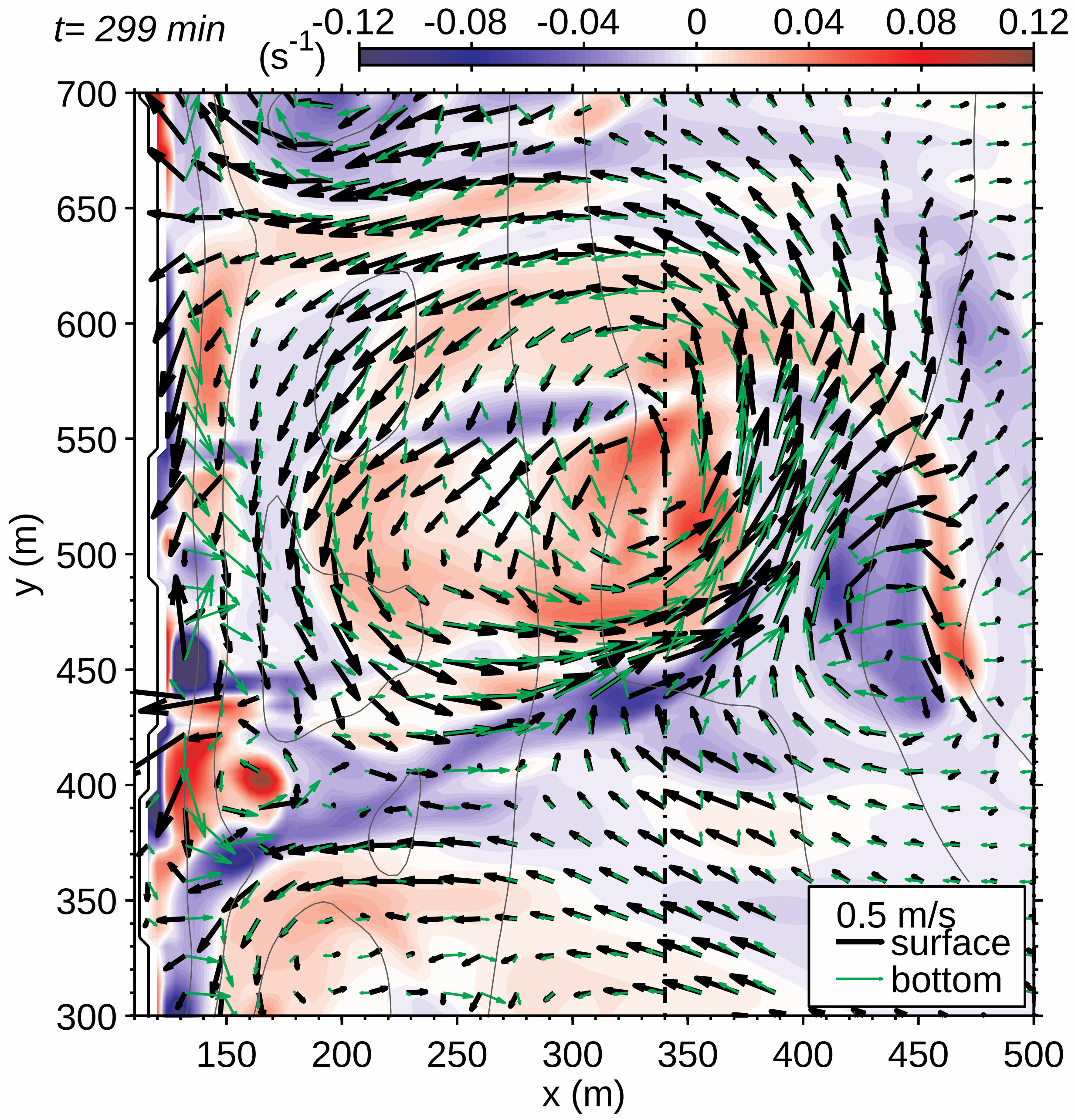

3D structure of littoral/rip currents (snapshot)

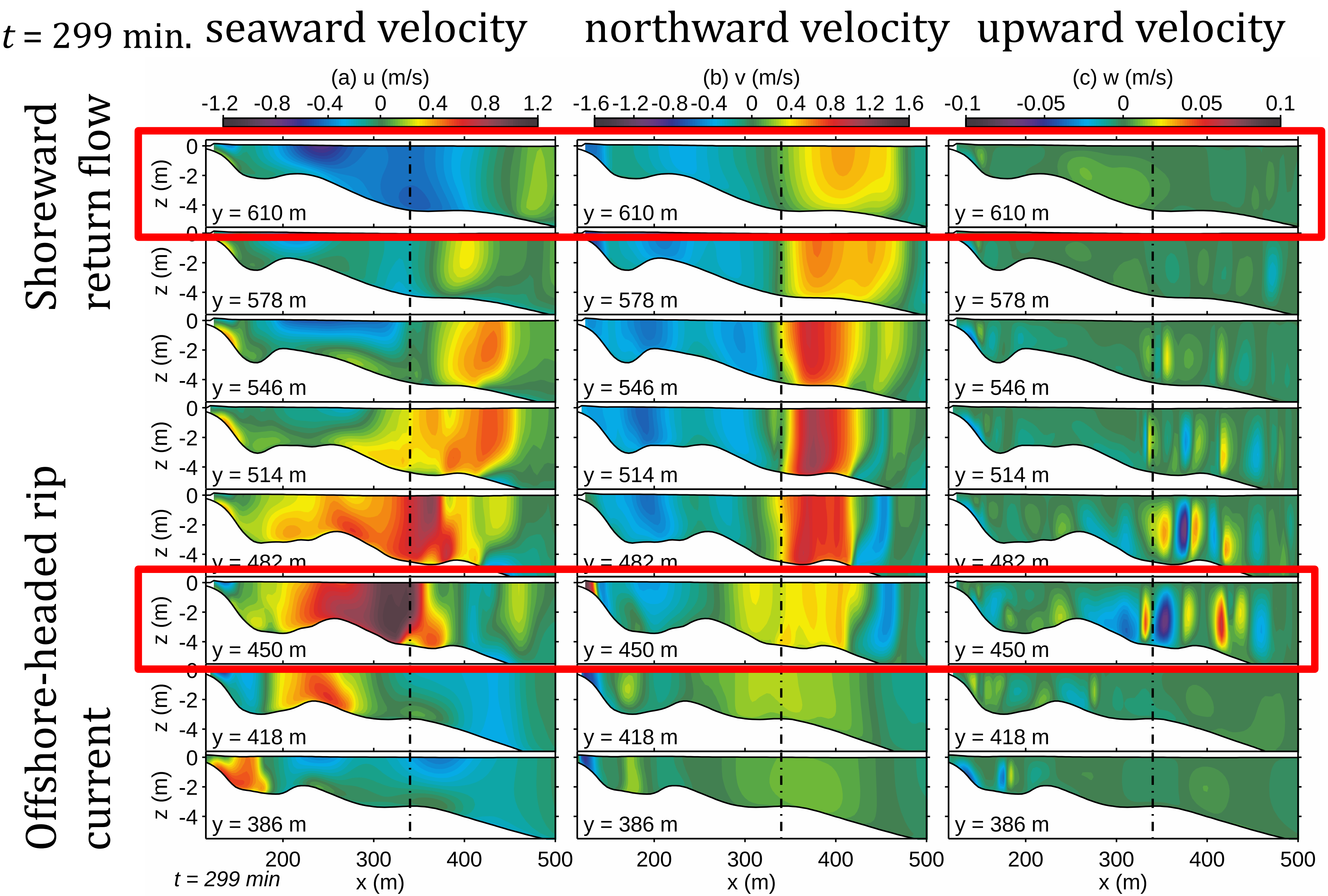

VLFs (very low frequency motions) under steady waves

- Definition of VLFs: e.g., McMahan et al. (2004)
- Reniers *et al*. (2008): infragravity group forcing
- Spydell and Feddersen (2009): phase-resolved irregular waves → *forced VLFs*
- Peaks at 8 x 10^{-4} Hz (20 min) and 3 x 10^{-4} Hz (55 min) in the PSD and the velocity time series→ *intrinsic VLFs*
- A band-pass filter is applied to extract the periods

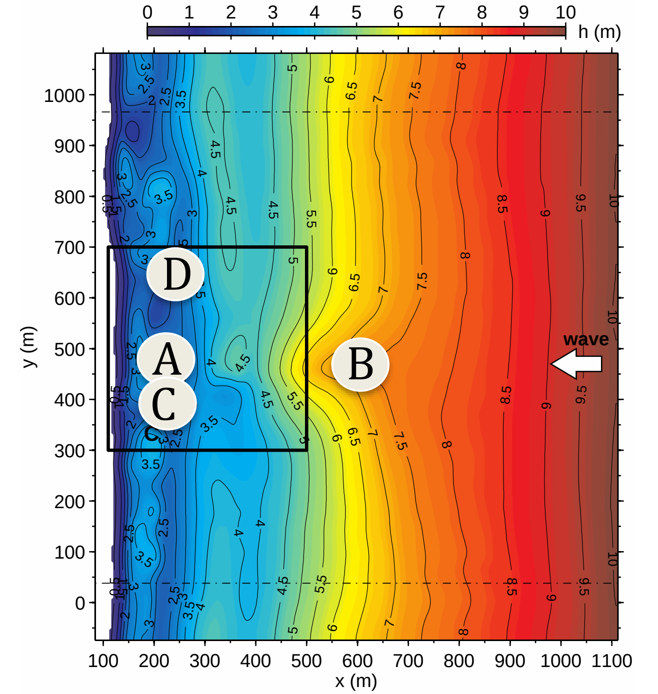

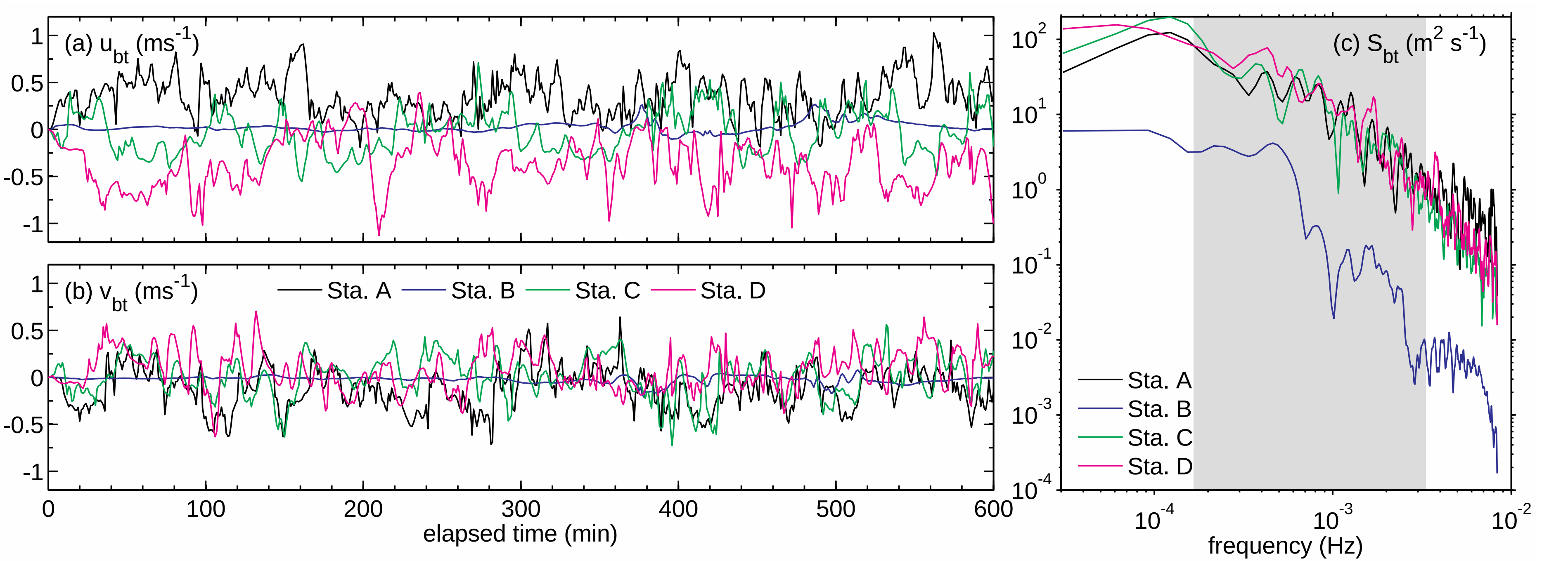

Wave-current interaction & three-dimensionality in VLFs

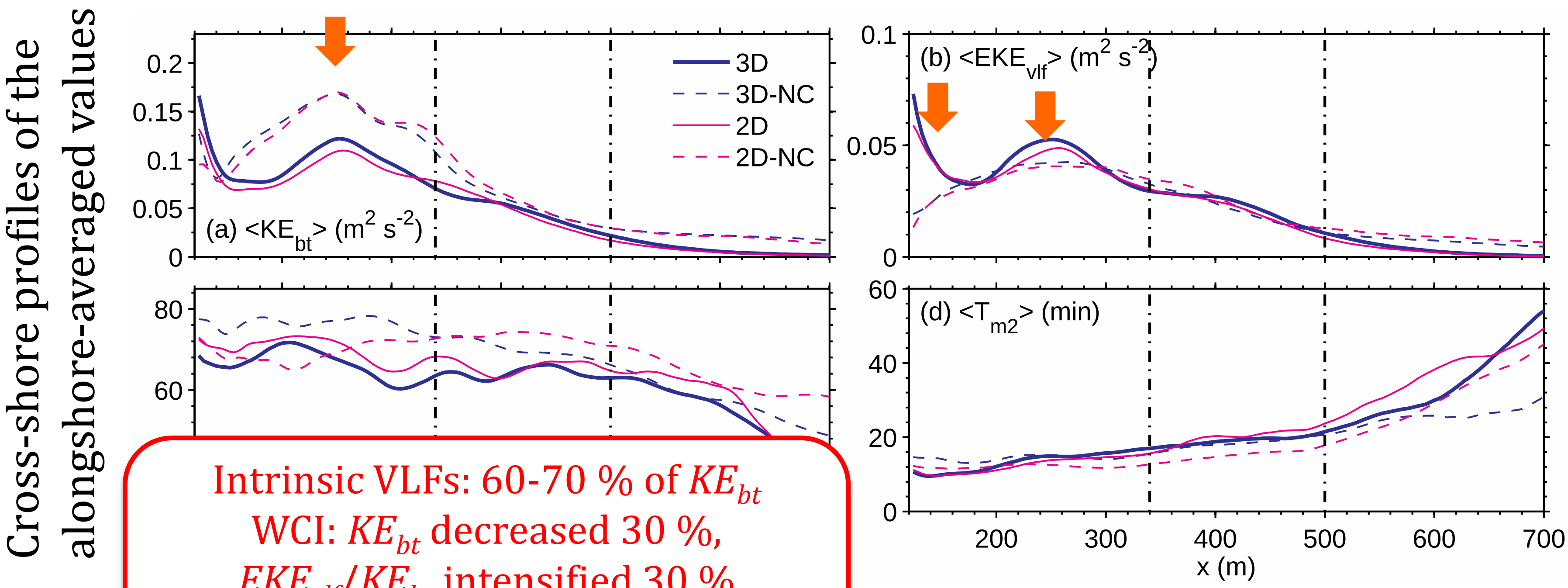

Intrinsic VLFs: 60-70 % of KE_{bt}
WCI: KE_{bt} decreased 30 %,
EKE_{vlf}/KE_{bt} intensified 30 %
2D vs. 3D: trivial
period (T_{m2}): 15-18 min.→ VLFs

variables plotted in **Fig.** averaged for *x* £ 600 m.

	3D	3D-NC	2D	2D-NC	unit
KE_{bt}	6.25	8.49	5.75	8.54	10^{-2} m^{2}s^{-2}
EKE_{tot}	4.28	3.45	3.83	3.67	10^{-2} m^{2}s^{-2}
EKE_{vlf}	2.80	2.53	2.62	2.58	10^{-2} m^{2}s^{-2}
T_{m2}	17.9	17.7	18.9	15.4	min
EKE_{tot}/KE_{bt}	71.9	46.1	69.5	49.2	%
EKE_{vlf}/KE_{bt}	46.1	32.2	46.5	34.4	%
EKE_{vlf}/EKE_{tot}	64.3	71.1	67.1	70.1	%

NC stands for
no interaction

Alongshore bathymetric variability (α in x) vs. VLFs

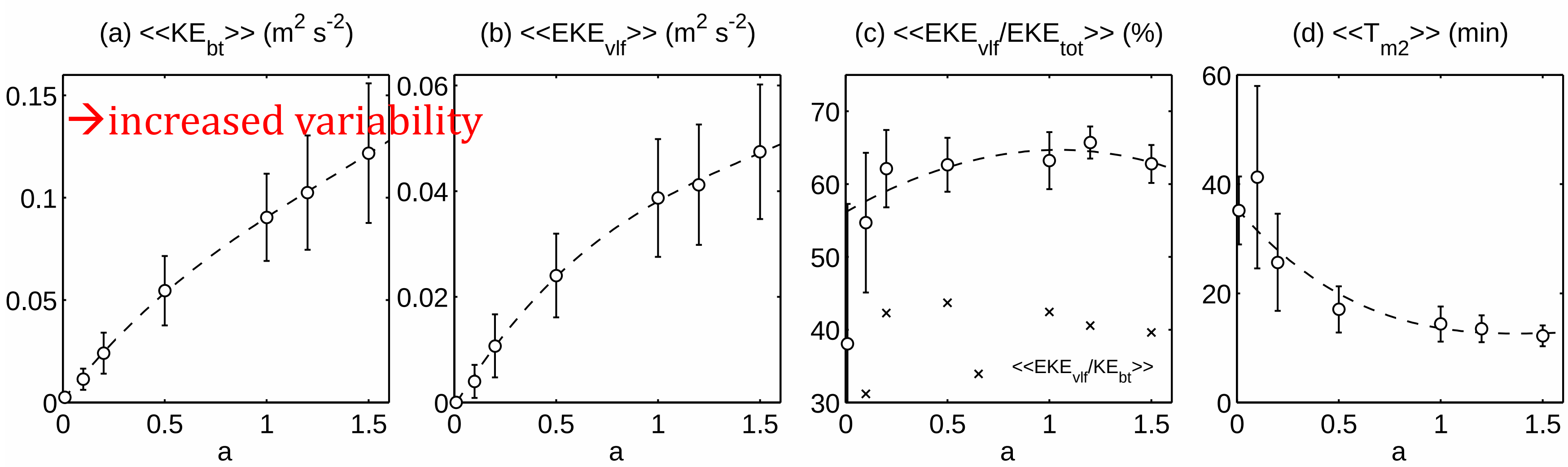

Offshore wave height (H_{rms} in x) vs. VLFs

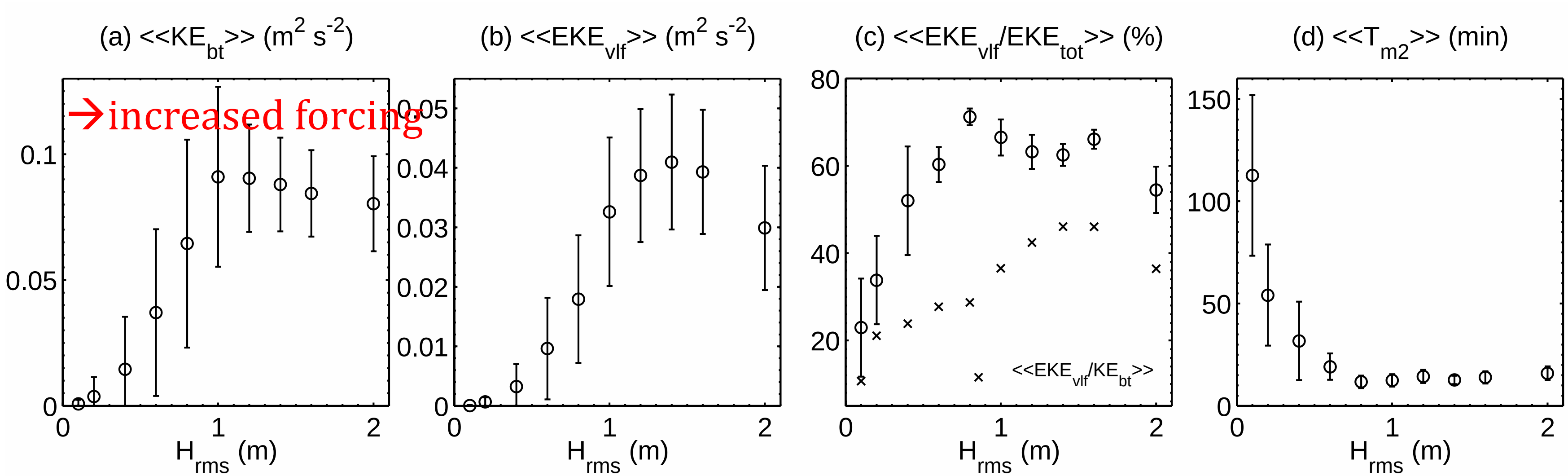

→ Consistent with *in situ* measurement (MacMahan *et al*., 2010)

spin-down test : decay of 3D turbulent rip eddies

Sequential decay of barotropic vorticity. Upper: 2D, lower: 3D

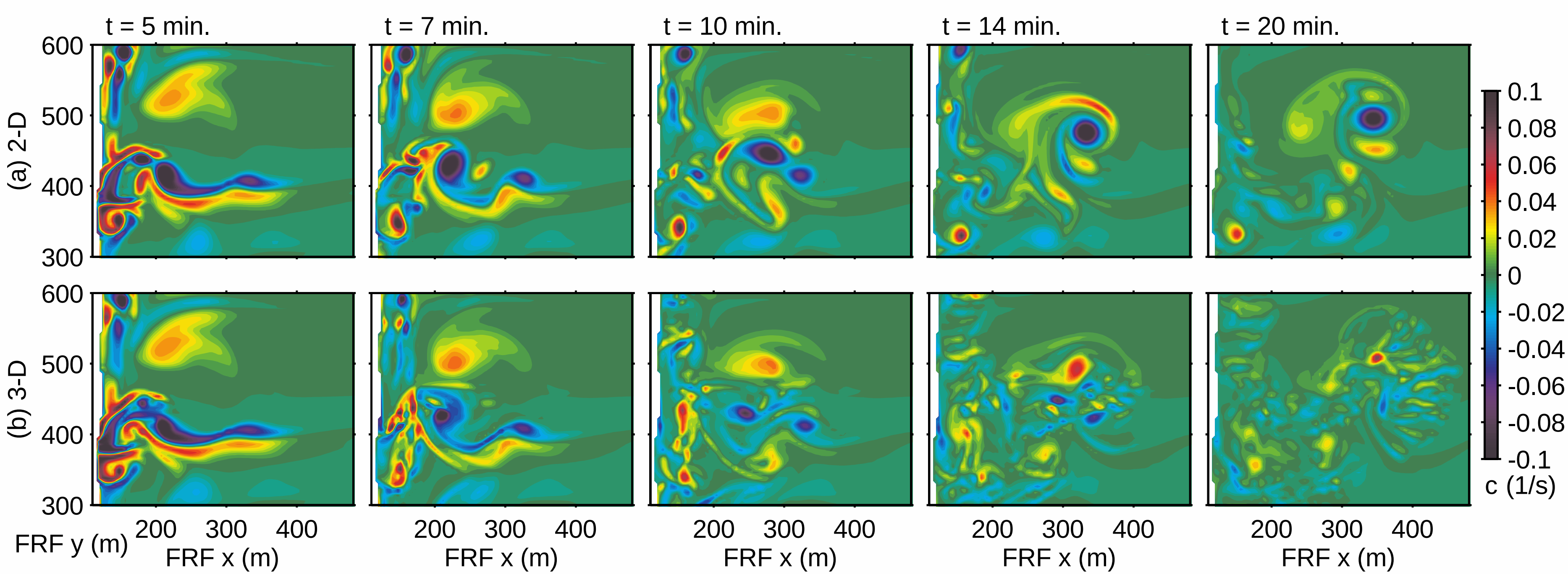

→ time

spin-down test

t < 5 min. energize turbulent rip with wave forcing imposed.

t > 5 min. turn off forcing to let the eddies decay

n.b., 2D case: 3D, but with a large background vertical eddy viscosity to virtually eliminate depth-dependency.

spin-down test : decay of 3D turbulent rip eddies

Unforced 3-D vorticity eq. ($f = 0$, ρ = const.)

$$\underbrace{\partial_t \omega_z}_{\text{tendency}} \underbrace{+(\mathbf{u}\cdot\nabla)\omega_z}_{\text{advection}} = \underbrace{\omega_x \partial_x w + \omega_y \partial_y w}_{\text{vortex tilting}} \underbrace{-\omega_z\left(\partial_x u + \partial_y v\right)}_{\text{vortex s}} \underbrace{+\partial_z\left(K_v \partial_z \omega_z\right)}$$

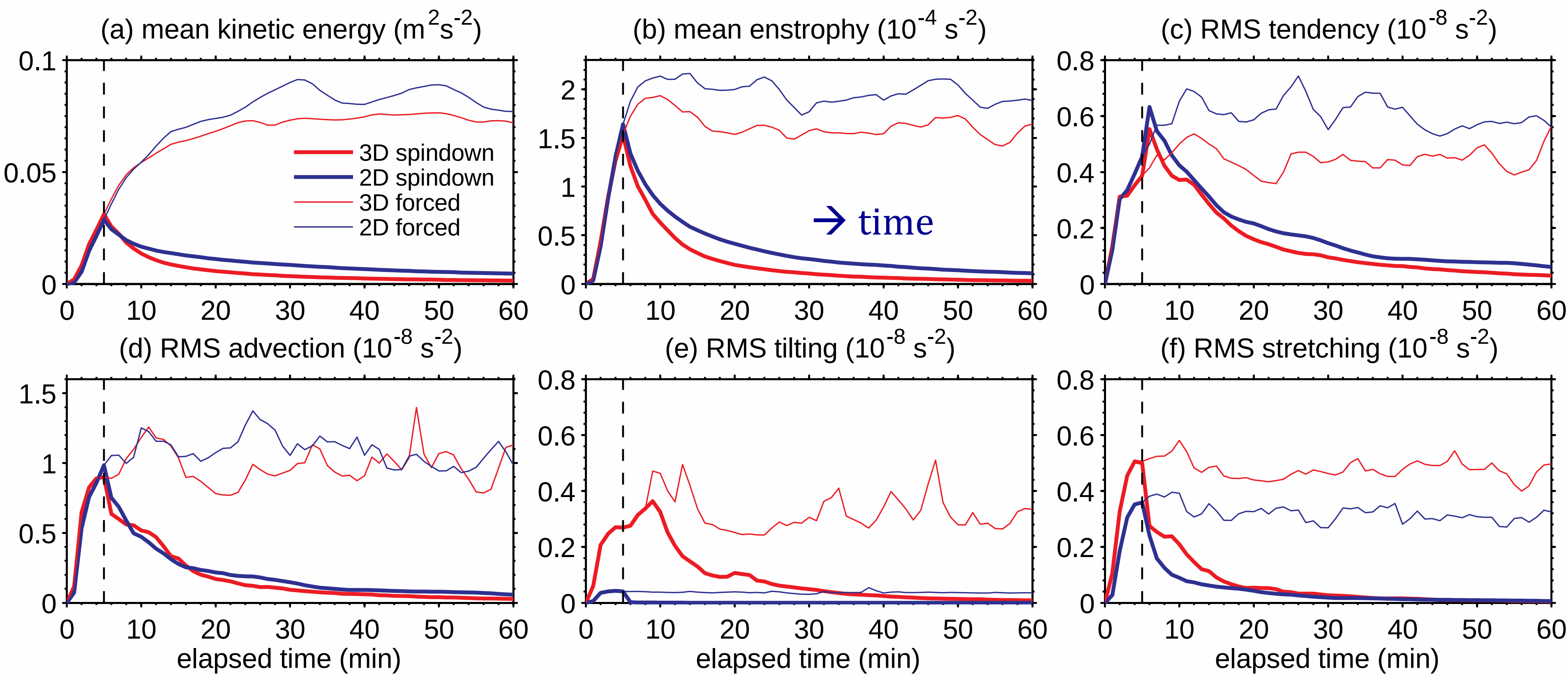

volume averaged over the entire domain

Innershelf-surf interaction

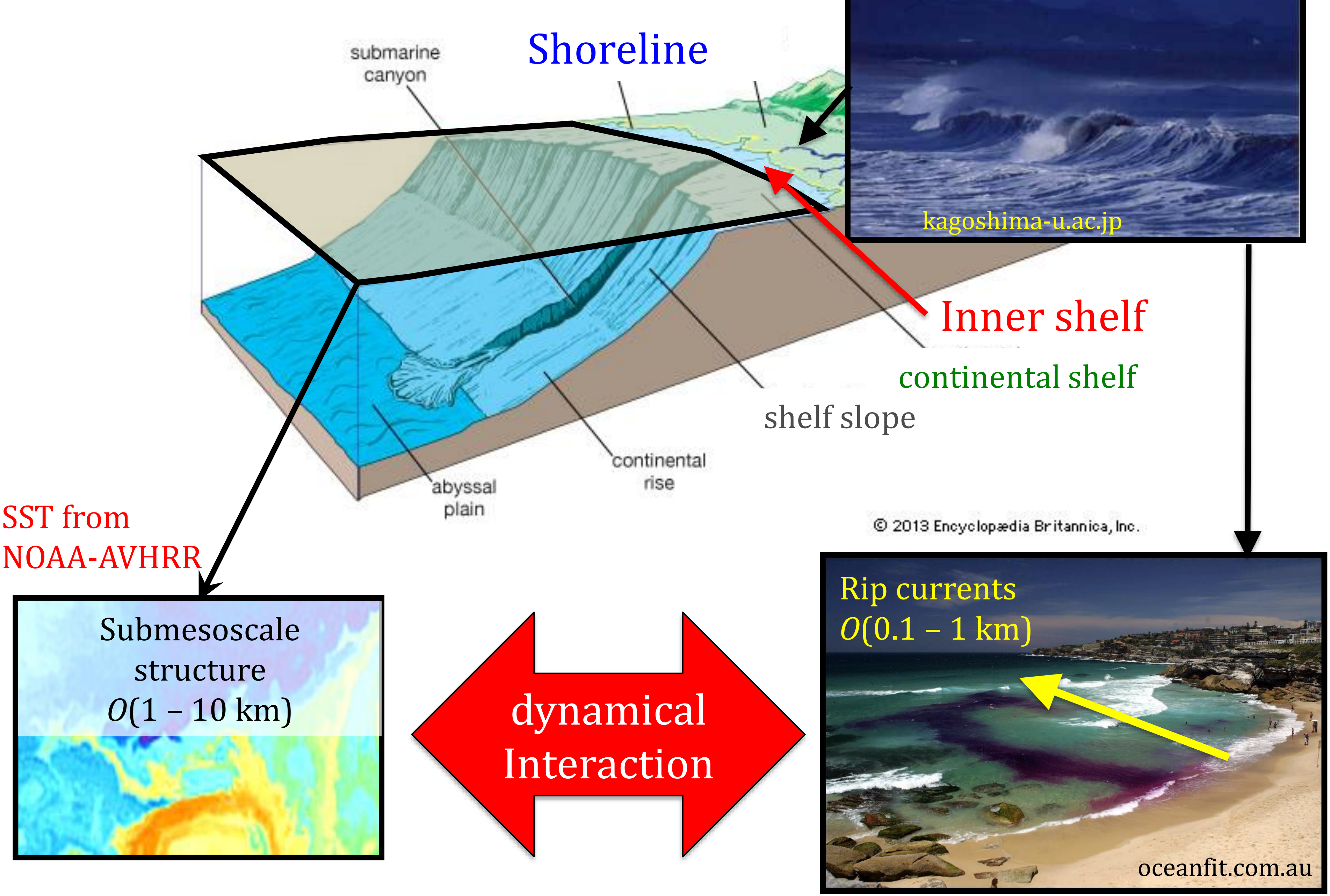

Submesoscale coherent structures (SCS) on the inner-continental shelf off California, U.S.

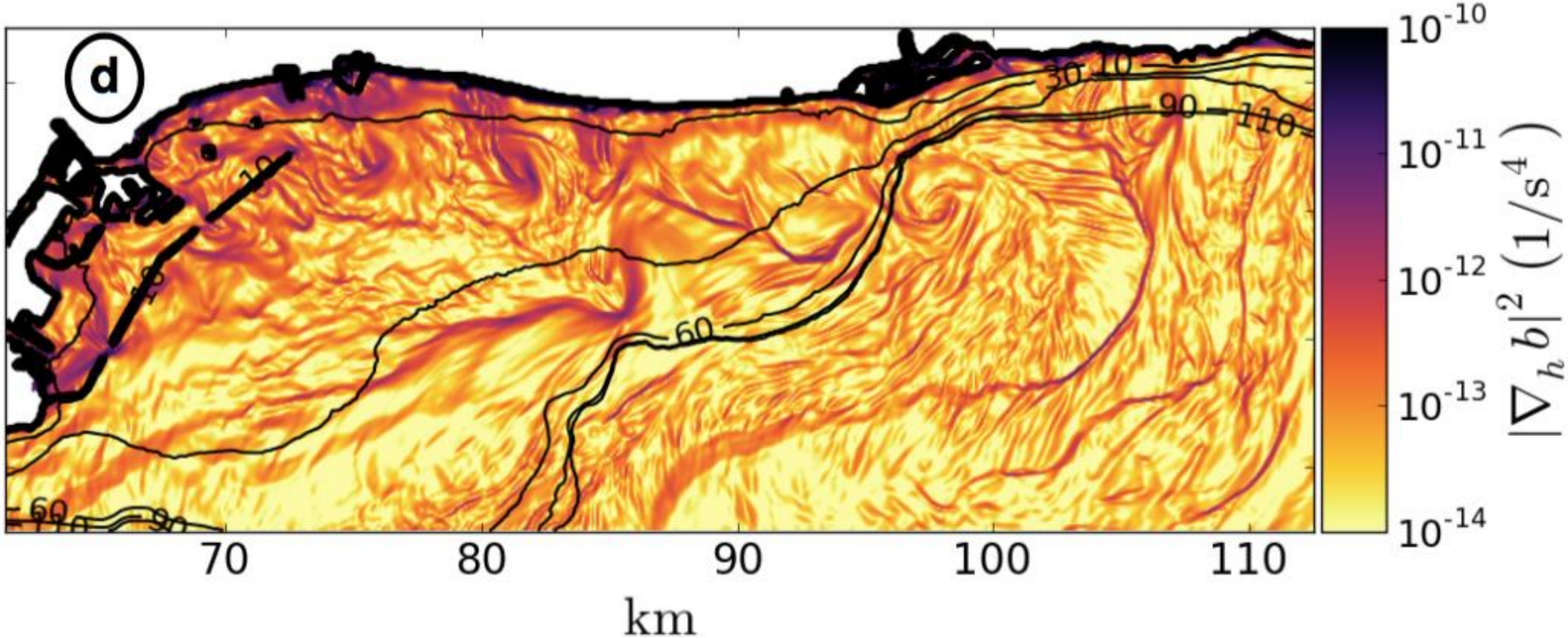

Snapshot of surface buoyancy gradient squared [Dauhajre, McWilliams and Uchiyama, 2017, JPO]

Question: How do surface gravity waves influence on SCSs and associated mixing and dispersal? → SCSs in idealized upwelling front is investigated with the ***ROMS-WEC*** [Uchiyama *et al*., 2010]

Idealized upwelling model configuration

Cross-shelf mean topography

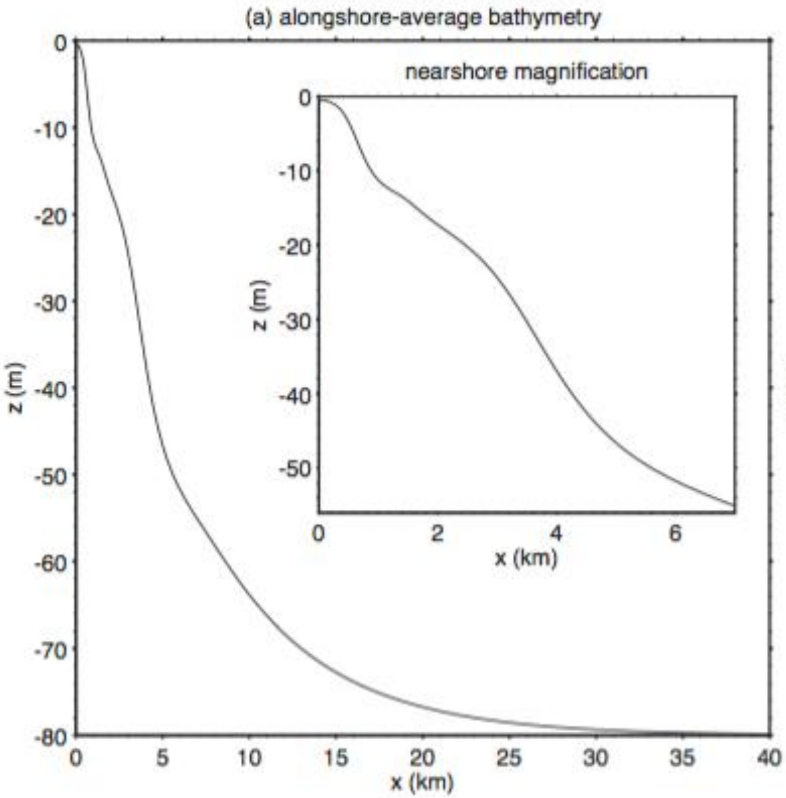

topography plan view

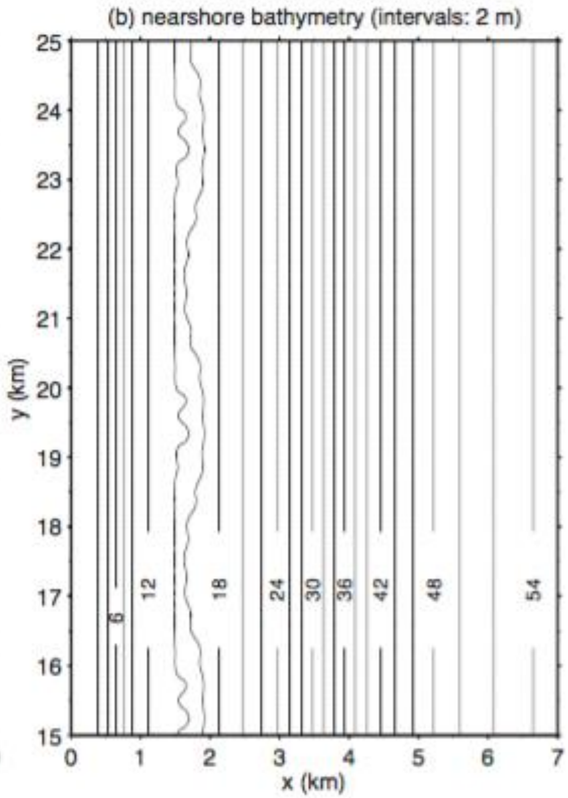

initial stratification

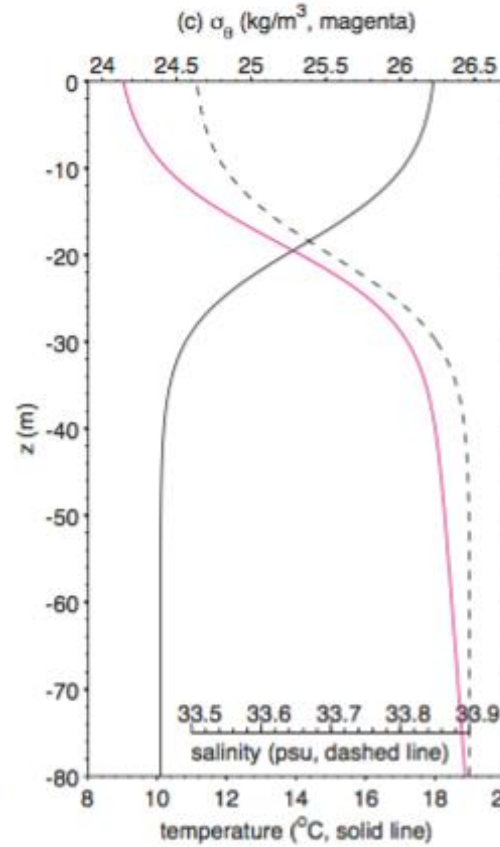

- Grid spacing: 80 m, 512 x 512 x 24 *s*-layers
- Start from the resting state.
- Two along-shelf topographic perturbations are added with along-shelf wavelengths of 512 and 4,096 m.

Idealized upwelling/downwelling configuration

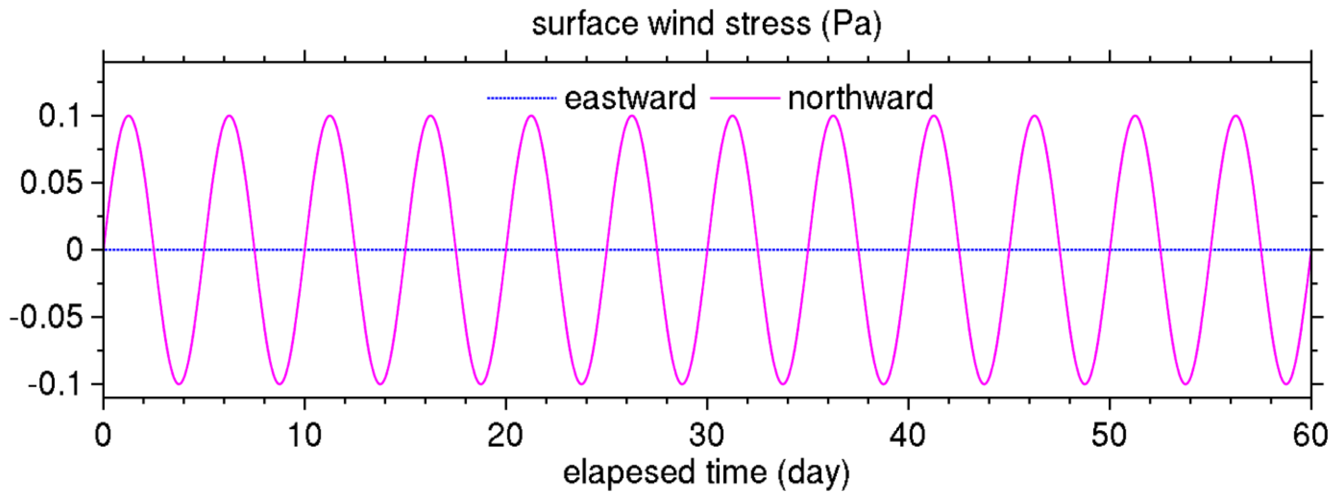

- Time-dependent alongshelf (y, northward) wind stress:

  $\boldsymbol{\tau} = (\tau_x, \tau_y) = (0, \tau_0 \sin[2p\ t/5]),$

  where t: days, τ_0 =0.1 [Pa].
- Positive t_y (northward) is upwelling favorable wind, which is then suppressed by negative, downwelling favorable wind.
- Incident waves (at the eastern open boundary)

  H_{rms} = 2A = 2.0 m, T_p = 7.0 s, q_p = 0^o (normal incidence)
- No surface heat/freshwater fluxes, leading to cooling/freshening with time (yet not so significant).
- Constant *f* (for the latitude around Santa Monica Bay), no beta effect
- Along-shelf periodic conditions

Surface potential density σ_θ [kg m^{-3}]

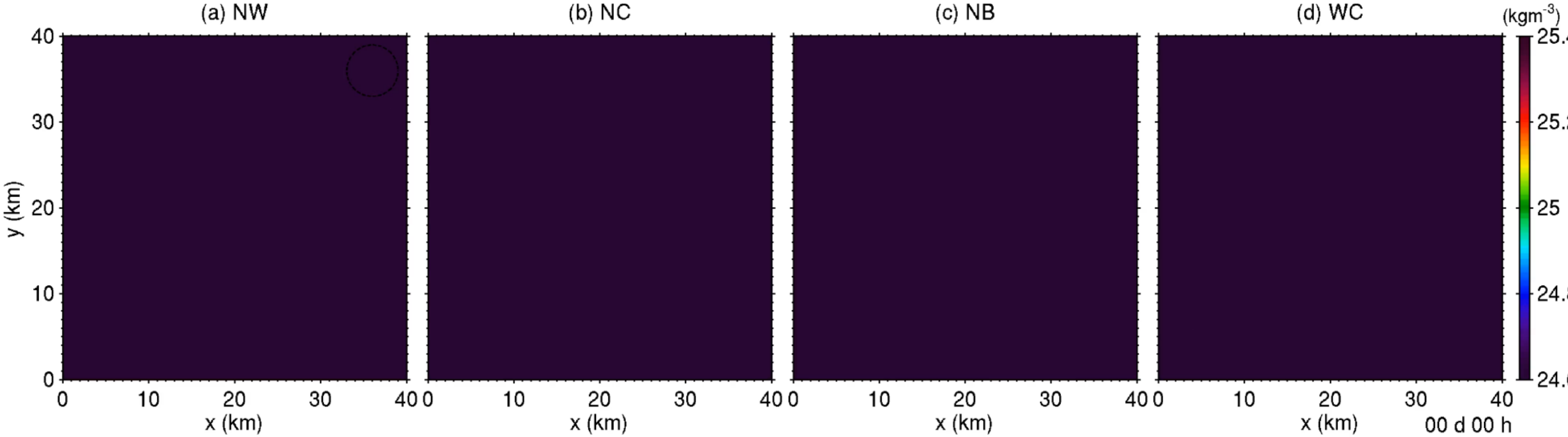

No wave WEC, no CEW WEC, no breaking WEC+CEW

Surface normalized relative vorticity [n.d.]

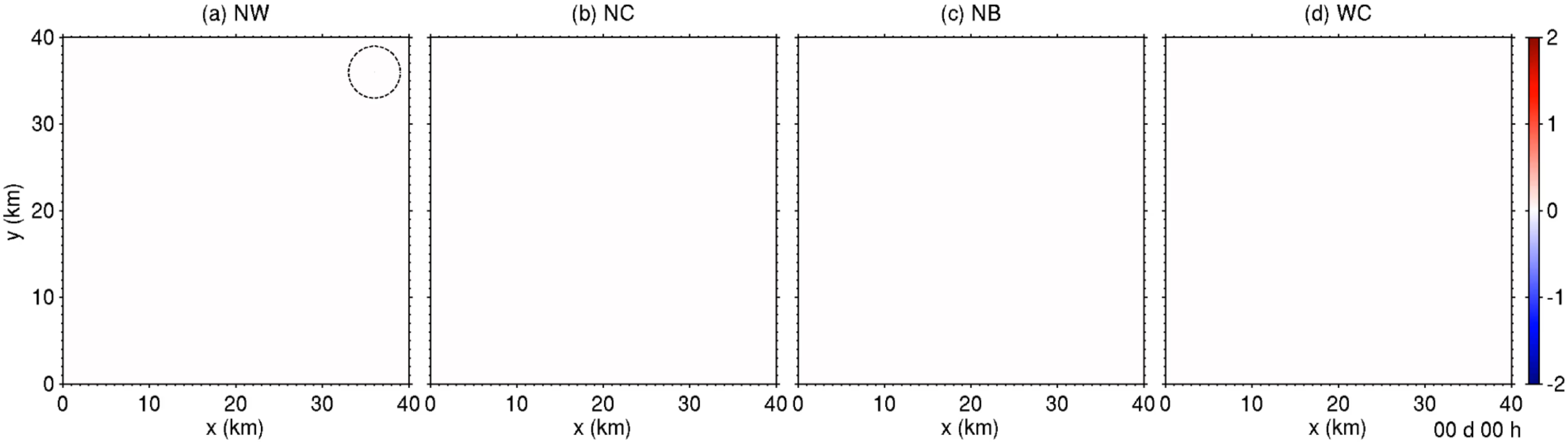

Surface enstrophy

Exclusion of WEC significantly reduces offshore surface enstrophy. NB is closer to WC/NC, so surf zone plays a minor role in altering offshore enstrophy.

offshore, x > 5 km

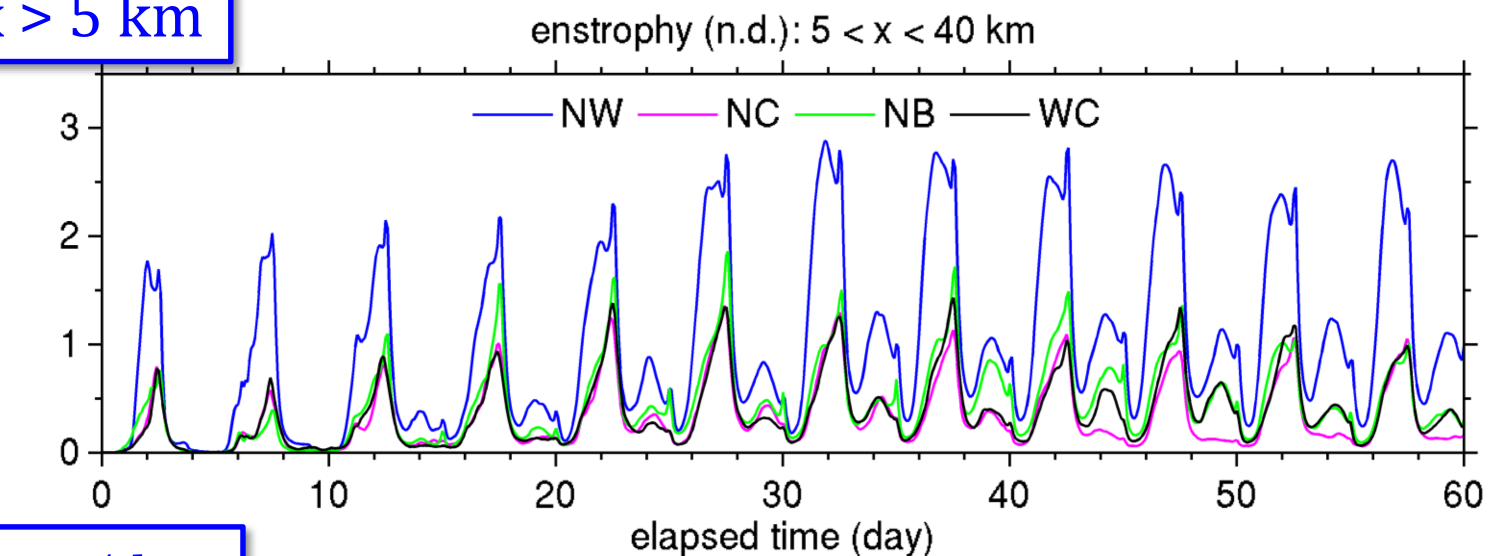

surfzone, x < 5 km

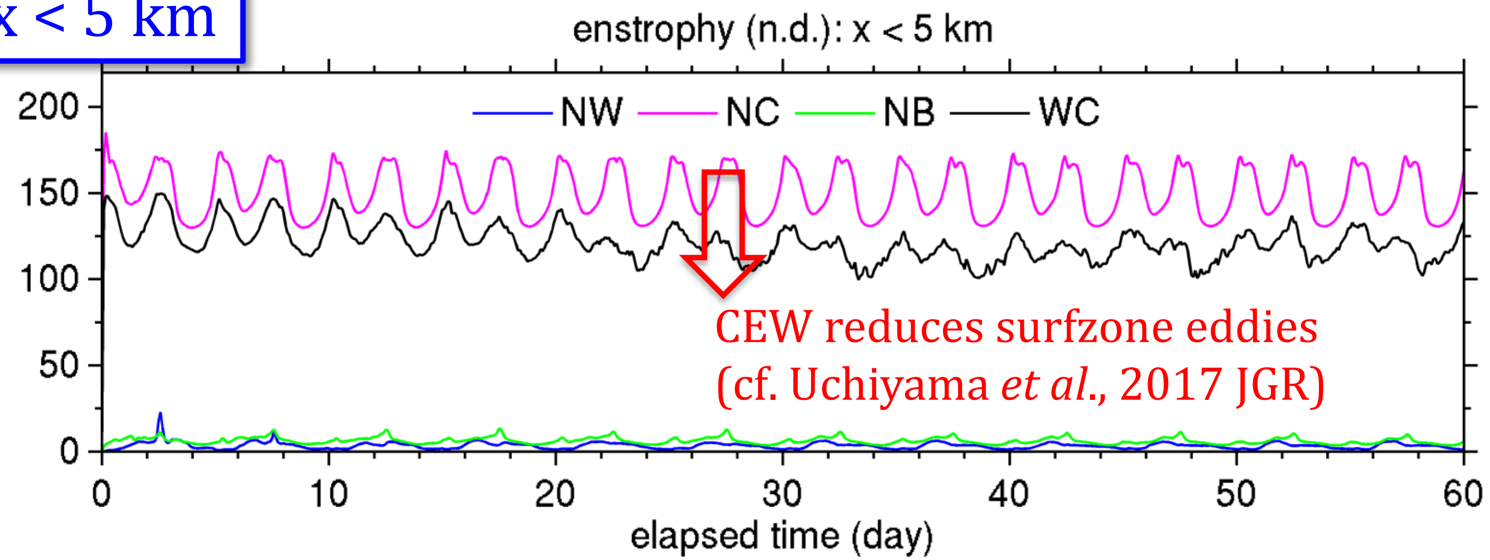

CEW reduces surfzone eddies (cf. Uchiyama *et al.*, 2017 JGR)

breaker acceleration largely intensifies enstrophy in the surf zone. CEW reduces it as expected (NC vs. WC).

Stokes-Ekman boundary layer

$$f\hat{\mathbf{z}}_3 \times (\mathbf{u} + \mathbf{u}_{st}) = \partial_z[\nu_v \partial_z \mathbf{u}]$$

$$\nu_v \partial_z \mathbf{u} = \frac{1}{\rho_0}\boldsymbol{\tau} \quad \text{at } z = 0$$

$$\partial_z \mathbf{u} = 0 \qquad \text{at } z = -H$$

Vertically-integrated transport

$$\mathbf{T}_\infty = \int_{-H}^{0} \mathbf{u}_\infty(z)\, dz = \hat{\mathbf{z}}_3 \times \frac{\boldsymbol{\tau}}{f\rho_0} - \int_{-H}^{0} \mathbf{u}_{st}\, dz$$

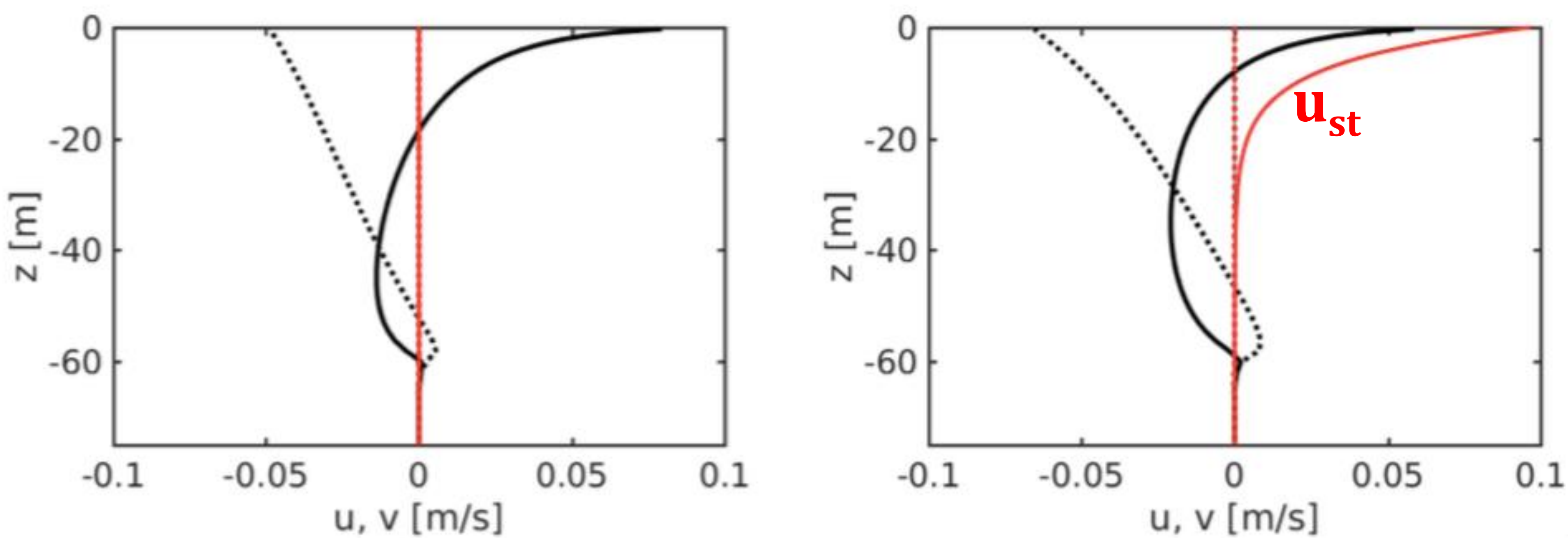

[after Xu and Bowen, 1994 JPO]

Boundary layer thickness matters?

[Time-average]

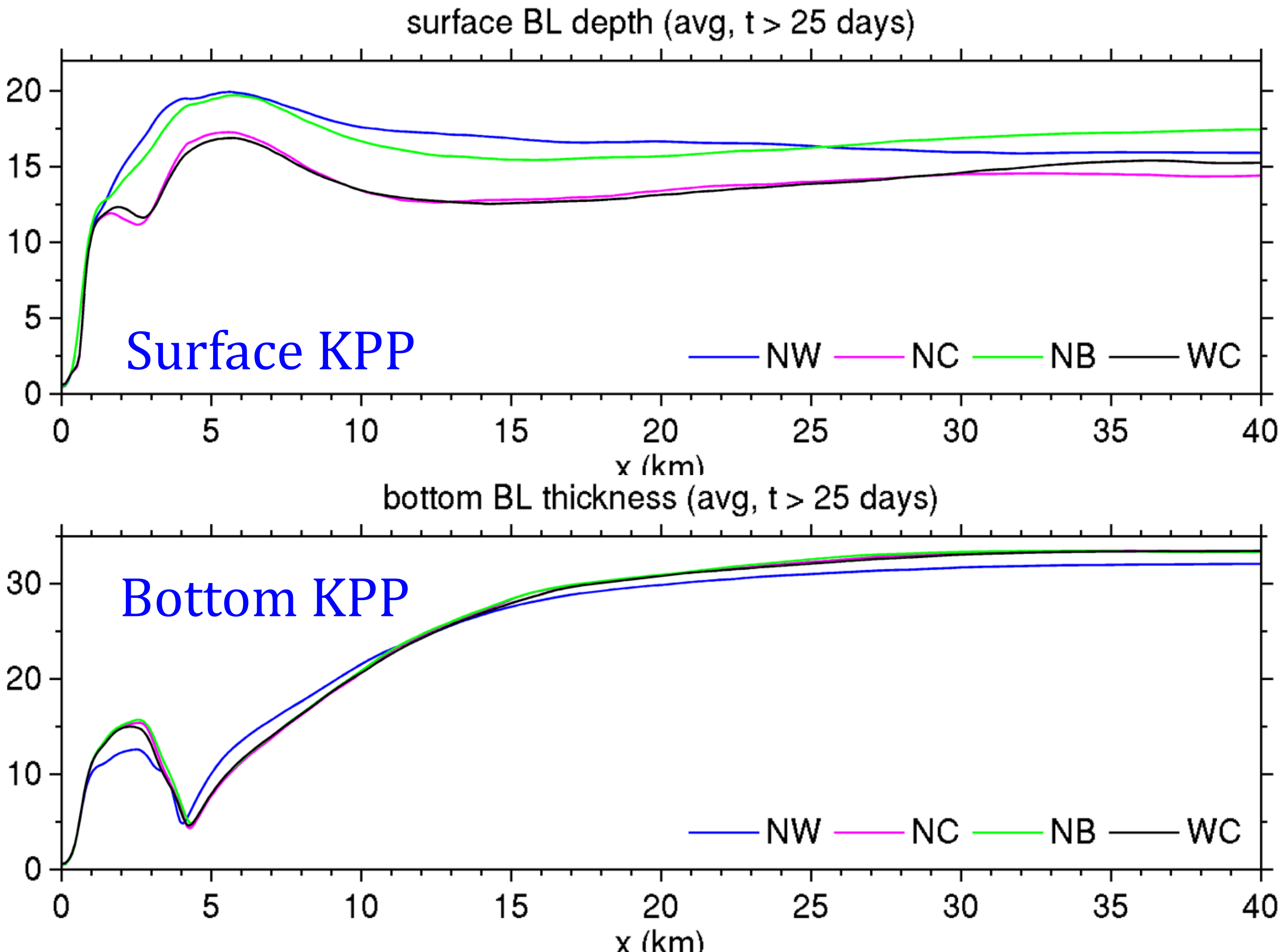

Surface MLD: NW=NB, NC=WC

Offshore K_v may differ by waves, although perhaps unrelated to enstrophy differences. Waves are insignificant for bottom BL thickness.

Frontogenetic tendency for the velocity gradient

$$D^L[\,\tfrac{1}{2}\,(\partial_i u^j)\,(\partial_i u^j)\,] \;=\; \mathcal{T}^{\mathbf{u}} \;=\; \mathcal{T}^{\mathbf{u}}_{a\,\phi} + \mathcal{T}^{\mathbf{u}}_{\nu_v} + \underline{\mathcal{T}^{\mathbf{u}}_{W}}$$

$$\mathcal{T}^{\mathbf{u}}_{W} \;=\; (\partial_j u^i) \int_{-H}^{z} \big(\, (\partial_z u^{st\,k})\,\partial_i\partial_j u^k \;+\; \underbrace{u^{st\,k}\,(\partial_i\partial_j\partial_k w)}_{\text{vortex-force contribution}}\,\big)\, dz$$

base line | reduced K_v

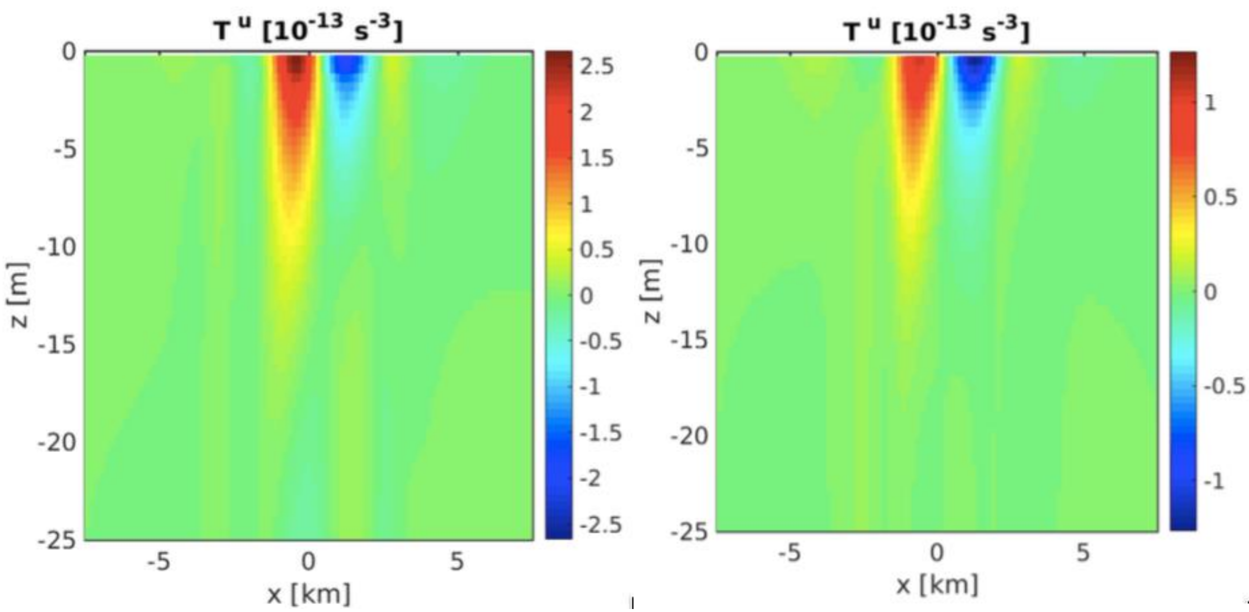

Waves diminish T^U through the Stokes advection (viz., cancelation of anti-Stokes flow) rather than the vortex-force contribution, in particular when K_v is small (e.g., weak wind)

[McWilliams, 2017, submitted to JFM]

Data Assimilation Seminar Series@RIKEN-AICS, Nov. 17, 2017

Challenges and issues in forward regional ocean modeling: Eddies, terrestrial influences, and surface gravity waves

Yusuke Uchiyama (Kobe University)

Visit our web site at http://coast.dce.kobe-u.ac.jp

Recent Publications

Dauhajre, D.P., McWilliams, J.C. and Uchiyama, Y. (2017): Submesoscale coherent structures on the continental shelf, J. Phys. Oceanogr., Vol. 47, doi:10.1175/JPO-D-16-0270.1

Uchiyama, Y., Kanki, R., Takano, A., Yamazaki, H. and Miyazawa, Y. (2017): Mesoscale reproducibility in regional ocean modeling with a 3-D stratification estimate based on Aviso-Argo data, Atmosphere-Ocean, doi: 10.1080/07055900.2017.1399858

Uchiyama, Y., McWilliams, J.C. and Akan, C. (2017): Three-dimensional transient rip currents: Bathymetric excitation of low-frequency intrinsic variability, J. Geophys. Res. Oceans, Vol. 122, pp. 5,826–5,849, doi:10.1002/2017JC013005.

Kamidaira, Y., Uchiyama, Y. and Mitarai, S. (2017): Eddy-induced transport of the Kuroshio warm water around the Ryukyu Islands in the East China Sea, Cont. Shelf Res., Vol. 143, pp. 206–218, doi:10.1016/j.csr.2016.07.004.

Uchiyama, Y., Suzue, Y. and Yamazaki, H. (2017): Eddy-driven nutrient transport and associated upper-ocean primary production along the Kuroshio, J. Geophys. Res. Oceans, Vol. 122, pp. 5,046–5,062, doi:10.1002/2017JC012847.

Romero, L., Siegel, D.A., McWilliams, J.C., Uchiyama, Y. and Jones, C. (2016): Characterizing stormwater dispersal and dilution from small coastal streams, J. Geophys. Res. Oceans, Vol. 121, doi:10.1002/2015JC011323.

Kumar, N., Feddersen, F., Suanda, S., Uchiyama, Y., McWilliams, J. and O'Reilly, W. (2016): Mid- to inner-shelf coupled ROMS-SWAN model-data comparison of currents, and temperature: Diurnal and semi-diurnal variability, J. Phys. Oceanogr., Vol. 46, pp. 841-862, doi:10.1175/JPO-D-15-0103.1

Marchesiello, P., Benshila, R., Almar, R., Uchiyama, Y., McWilliams, J. and Shchepetkin, A. (2015): On tridimensional rip current modeling, Ocean Modell., Vol. 96:1, pp. 36–48, doi:10.1016/j.ocemod.2015.07.003.

Kumar, N., Feddersen, F., Uchiyama, Y., McWilliams, J. and O'Reilly, W. (2015): Mid-shelf to surf zone coupled ROMS-SWAN model-data comparison of waves, currents, and temperature: Diagnosis of subtidal forcings and response, J. Phys. Oceanogr., Vol. 45, pp.1464–1490. doi: http://dx.doi.org/10.1175/JPO-D-14-0151.1.

Uchiyama, Y., Idica, E., McWilliams, J.C. and Stolzenbach, K.D. (2014): Wastewater effluent dispersal in Southern California Bays, Cont. Shelf Res., Vol. 76, pp. 36-52. doi:10.1016/j.csr.2014.01.002